WASHINGTON STATE HIGHWAY DEPARTMENT RESEARCH PROGRAM
REPORT 24.3

NOISE BARRIER SCREEN MEASUREMENTS

DOUBLE BARRIERS

RESEARCH PROJECT

Y-1663

AUGUST 1976

PREPARED FOR
WASHINGTON STATE
HIGHWAY COMMISSION

R. N. FOSS
APPLIED PHYSICS LABORATORY
UNIVERSITY OF WASHINGTON

TECHNICAL REPORT STANDARD TITLE PAGE

1. Report No.	2. Government Accession No.	3. Recipient's Catalog No.
24.3		

4. Title and Subtitle	5. Report Date
NOISE BARRIER SCREEN MEASUREMENTS , Double Barriers	August 1976
	6. Performing Organization Code

7. Author(s)	8. Performing Organization Report No.
Rene N. Foss	APL-UW 7618

9. Performing Organization Name and Address	10. Work Unit No.
Applied Physics Laboratory University of Washington 1013 N.E. 40th Seattle, WA 98105	11. Contract or Grant No. Y-1663
	13. Type of Report and Period Covered Program Report
12. Sponsoring Agency Name and Address Washington State Highway Commission Department of Highways Highway Administration Building Olympia, WA 98504	14. Sponsoring Agency Code

15. Supplementary Notes

This study was conducted in cooperation with the U.S. Department of Transportation, Federal Highway Administration.

16. Abstract

This report documents the results of an investigation to determine the attenuative effect of two cascaded walls or barrier screens on the transmission of sound. The study was for point sources and involved the use of tone burst techniques for the experimental determination of the attenuation produced by a wide variety of two-wall configurations. This work was modeled at 5 and 10 kHz. The final result was the development of an algorithm for accurately predicting the attenuation of two-wall systems.

17. Key Words	18. Distribution Statement
Noise suppression Noise barriers Noise screens Highway acoustics Fresnel diffraction	

19. Security Classif. (of this report)	20. Security Classif. (of this page)	21. No. of Pages	22. Price
Unclassified	Unclassified	43	

WASHINGTON STATE HIGHWAY DEPARTMENT RESEARCH PROGRAM REPORT **24.3**

NOISE BARRIER SCREEN MEASUREMENTS

DOUBLE BARRIERS

RESEARCH PROJECT

Y-1663

AUGUST 1976

PREPARED FOR
WASHINGTON STATE
HIGHWAY COMMISSION

R. N. FOSS
APPLIED PHYSICS LABORATORY
UNIVERSITY OF WASHINGTON

The opinions, findings and conclusions expressed in this publication are those of the authors and not necessarily those of the Washington State Highway Commission, Department of Highways or the Federal Highway Administration.

TABLE OF CONTENTS

ABSTRACT

This report documents the results of an investigation to determine the attenuative effect of two cascaded walls or barrier screens on the transmission of sound. The study was for point sources and involved the use of tone burst techniques for the experimental determination of the attenuation produced by a wide variety of two-wall configurations. This work was modeled at 5 and 10 kHz. The final result was the development of an algorithm for accurately predicting the attenuation of two-wall systems.

INTRODUCTION

The study reported here was undertaken for the State of Washington Department of Highways to find a calculation procedure, or algorithm, that would accurately predict the effect of two cascaded walls.

Extensive experiments with double walls conducted as part of this work have shown that double walls are more effective at blocking sound than they are being given credit for, particularly if the theory referred to in this report as the "leaning pole" theory is relied on for predictive purposes. This theory, which is not, of course, universally known by the name "leaning pole," assumes that the effect of the double wall can be calculated by substituting a single wall with a specific height and placement determined as follows: A straight "pole" is laid from the noise source over the top of the adjacent wall in line with the receiver as shown in Figure 1. Then another straight "pole" is laid from the receiver toward the noise source so that it leans up against its adjacent wall. In most cases, these poles will cross at some point. The theory assumes that a single wall with its top exactly where these two poles cross would produce the same total acoustic attenuation as the two individual walls. This model has some validity in that it at least predicts that where both walls block the line of sight the two walls will produce more attenuation than either of the walls considered singly. This method, however, has been criticized because for many simple (but extreme) cases it is obviously faulty. If, for example, the source and the receiver are both very close to their adjacent walls, the angle of the poles is so steep that they cross at an extremely high altitude (see bottom sketch of Figure 1); a single wall of this height would yield much more attenuation than that actually produced by the two walls. In addition, the theory cannot handle at all those cases where one wall is above the source-receiver line of sight and the other is below it.

Although for the extreme case cited above the attenuation predicted by the leaning pole theory tends to be much higher than what would actually occur, our experiments showed that, for a wide range of conditions more likely to occur in highway noise suppression work, the leaning pole theory rather consistently under predicts the amount of attenuation that the two walls would actually produce. Figures 2 through 5 show the attenuation actually produced by a two-wall configuration plotted as a function of the height of the source and the receiver where the relative spacing of the source, walls, and receiver is fixed. Also plotted on the graphs is the attenuation that would be predicted by the leaning pole theory for the same geometries, along with the attenuation predicted by the final algorithm developed as a result of this study. As can be seen, the leaning pole theory considerably under predicts the attenuation, at one point (in Figure 3) by as much as 11 dB.

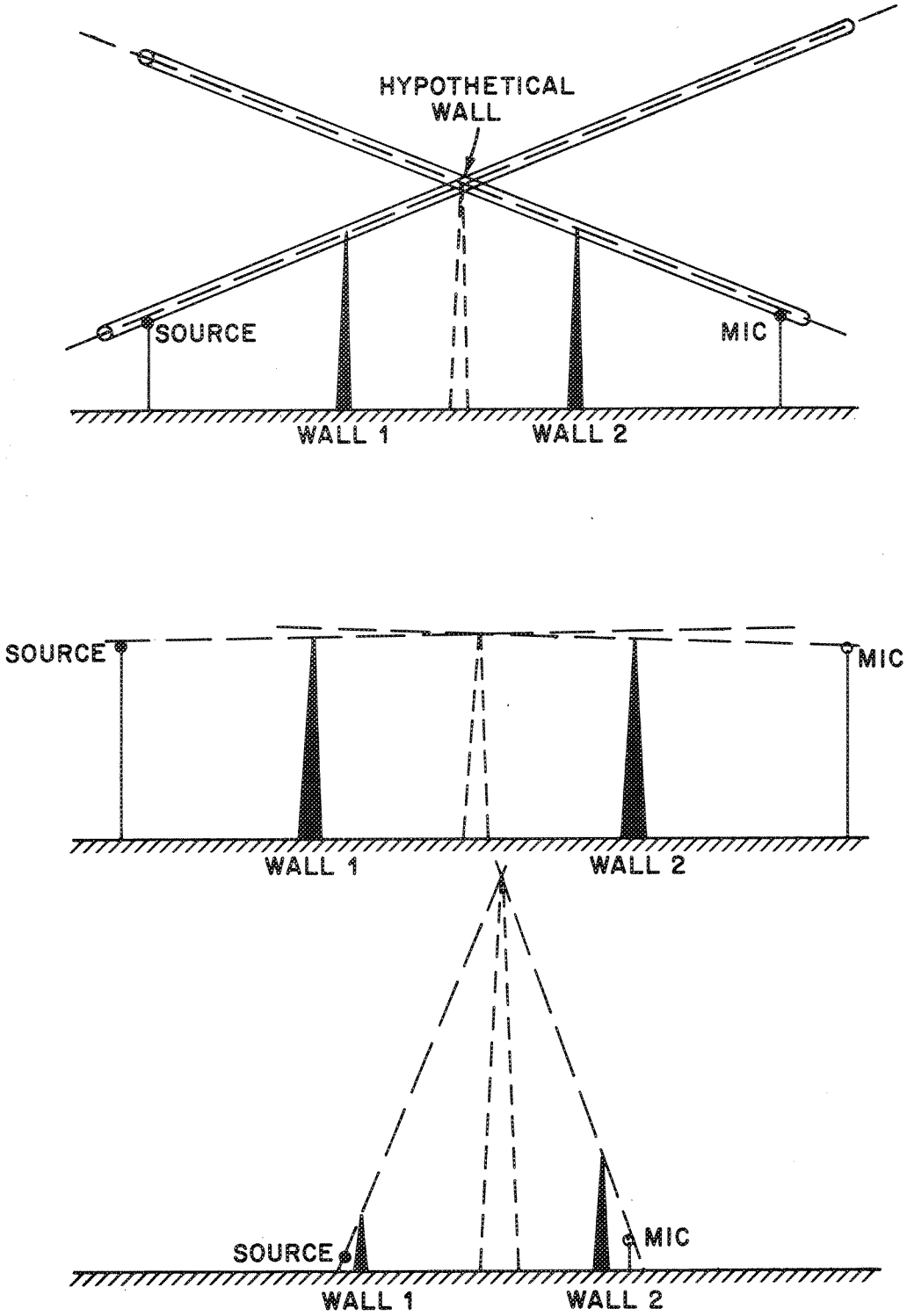

Figure 1. Leaning pole theory geometry.

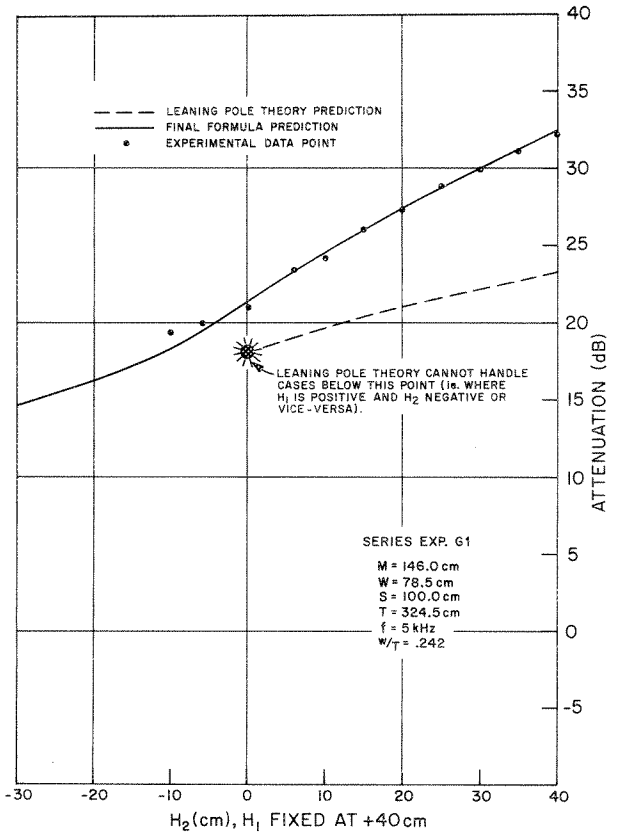

Figure 2. Sample of leaning pole theory underprediction. (See pp. 9 and 16 for explanation of M, W, etc.)

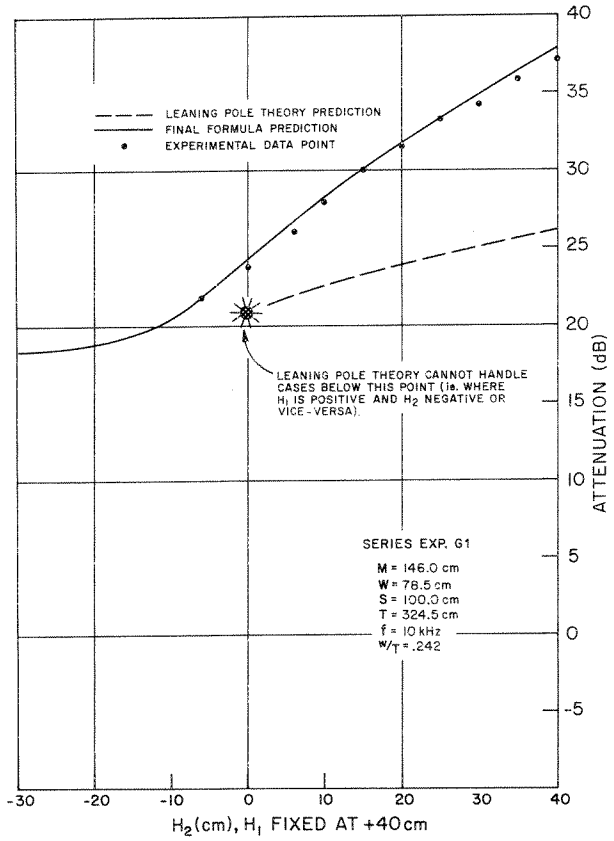

Figure 3. Sample of leaning pole theory underprediction.

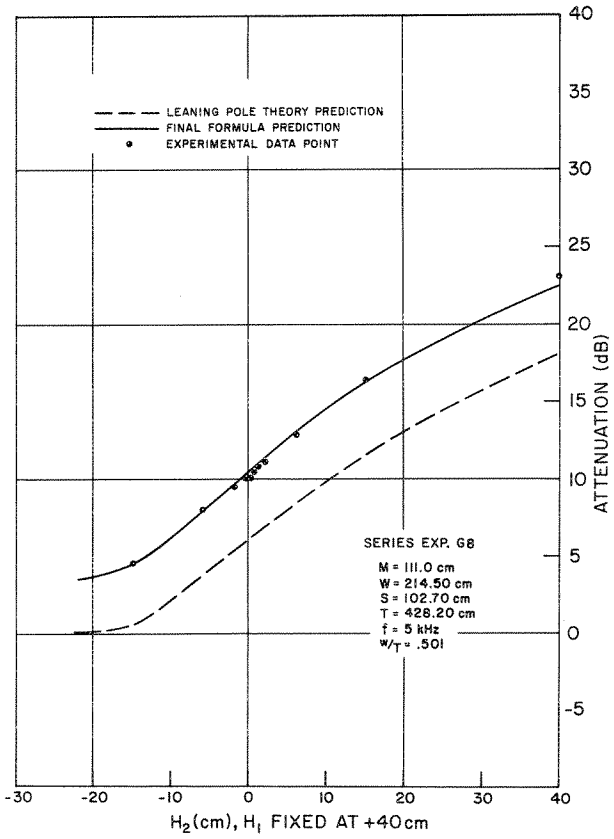

Figure 4. Sample of leaning pole theory underprediction.

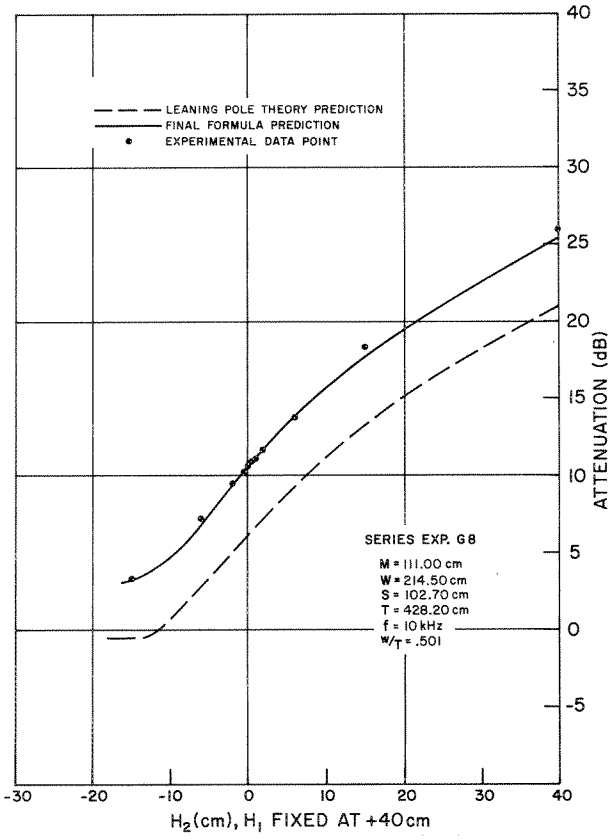

Figure 5. Sample of leaning pole theory underprediction.

The net result of this underprediction has been that double walls are not normally considered seriously for noise abatement schemes. This does not mean that the erection of a second wall would be the economical way to proceed in all cases where more attenuation is desired than would be produced by a proposed single wall. Other alternatives (building the first wall higher, moving the noise source farther away, etc.) should be investigated. However the algorithm developed in this study as a result of a careful experimental effort should enable two-wall alternates to be properly considered. In addition, there are times when other alternatives are not available--such as, for example, when a land developer wishes additional protection and does not have the option of moving the road or increasing the height of the existing wall. With this algorithm, the effect of constructing a new wall can be predicted.

MEASUREMENT OF DATA

There were, of course, a number of criteria that needed to be met in order to create a viable algorithm with general utility. These included carrying out the experiments at at least two frequencies (see p. 9), taking accurate measurements of the exact geometries involved, and determining the experimental attenuation accurately enough that scatter in the data did not becloud the actual phenomena taking place.

Procedure

The measurement apparatus and experimental procedure were basically the same as those described in APL-UW 7509, "Noise Barrier Screen Measurements, Single Barriers" (Research Report No. 24.1, Washington State Department of Highways), dated June 30, 1975, and the reader is referred to that document for a full amplification of the experimental procedures and apparatus, and discussion of many of the small sources of experimental error that could be involved in the measurements. For the convenience of readers not having that report immediately available, the section on measurement procedures is reproduced in Appendix C.

Two-Wall Attenuation Measurements

Figures 6 and 7 are photographs of the two-wall setup and Figure 8 is a drawing showing the geometrical relationships for the tests conducted. For each geometric spacing, we first determined the attenuation produced by the wall nearer the source by carefully measuring the signal when the wall was raised and when it was lowered. The attenuation produced by the second wall by itself was then carefully determined by measuring the signal level with that wall raised and then lowered. Finally, the attenuation of the two walls together was obtained by measuring the signal

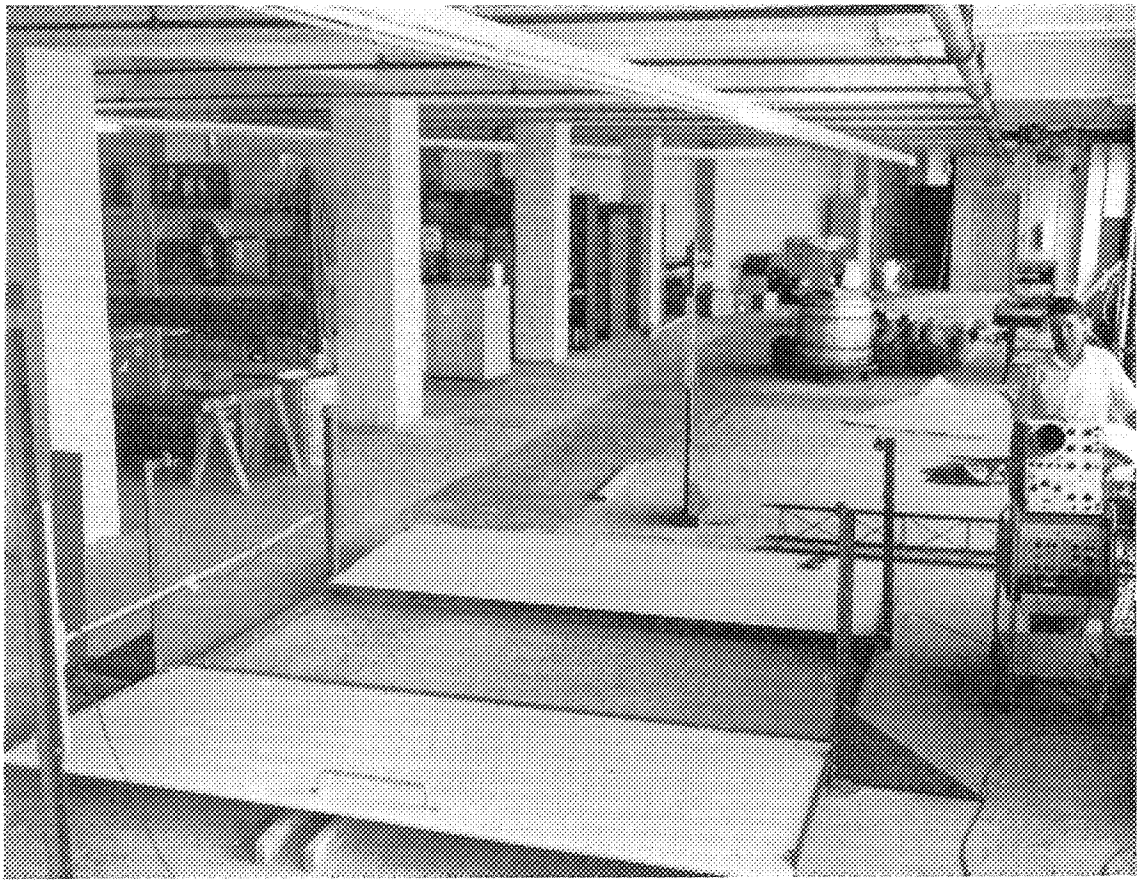

Figure 6. Photograph of measurement setup with both walls down.

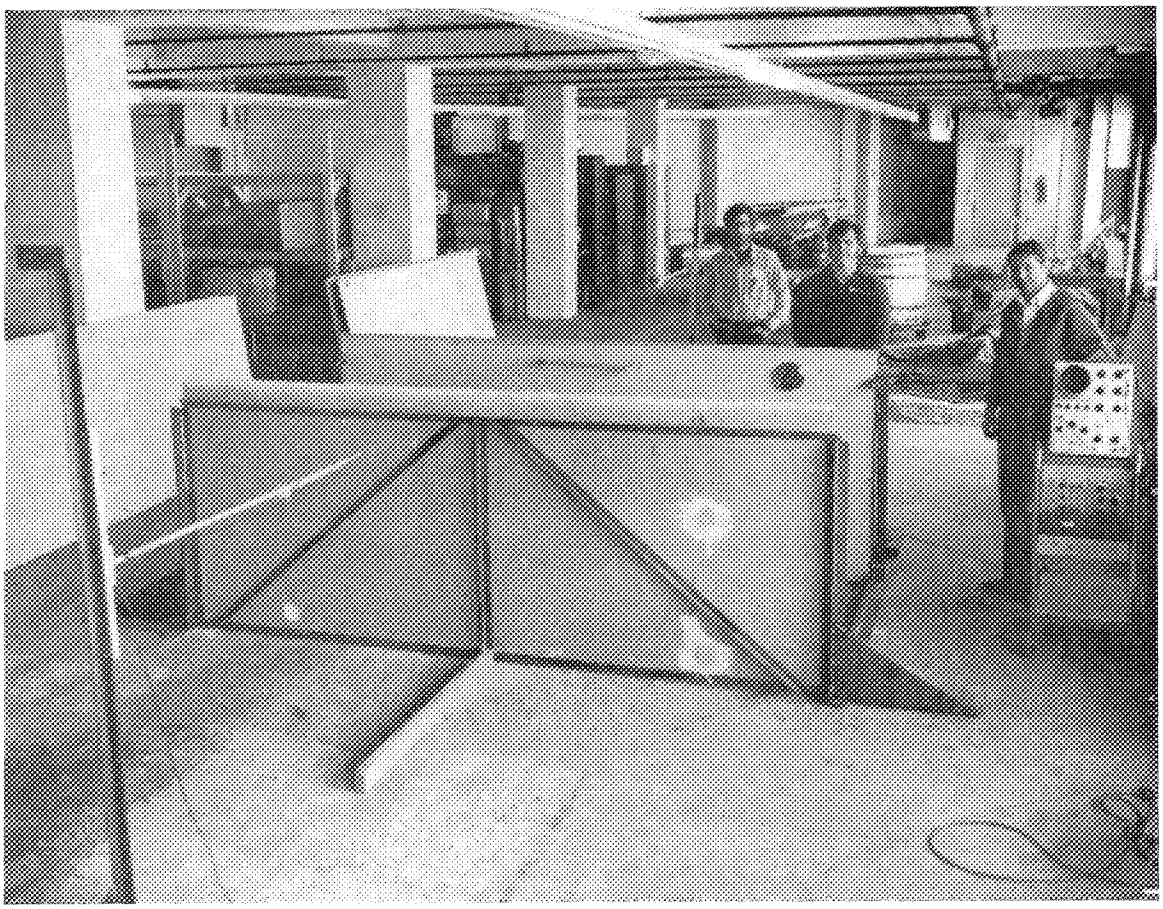

Figure 7. Photograph of measurement setup with both walls up.

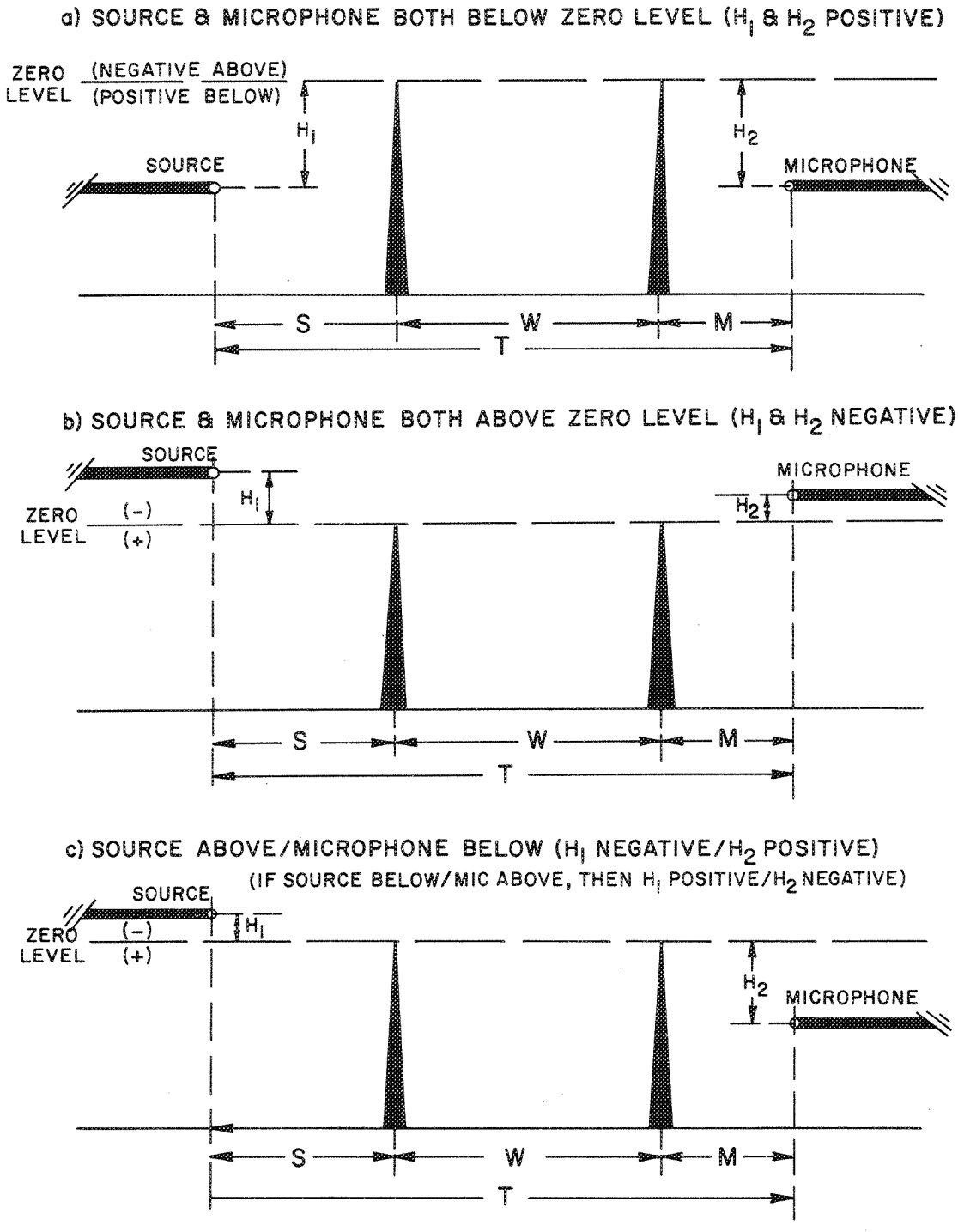

Figure 8. Geometrical relationship for experimental setup.

level when both walls were down vis-à-vis when they were up. These measurements were then repeated for a variety of source and microphone heights varying from 40 cm below the tops of the walls to 40 cm above them and for a variety of wall spacings and source-to-microphone spacings (see Table I).

For each test condition, the geometric positions of the source, the two walls, and the microphone were all carefully measured using the same exactness described in APL-UW 7509. As with the single-wall case, it was not practical to change the actual height of the wall vis-á-vis the floor of the building and the equivalent physical effects were obtained by independently varying the heights of the source and the microphone. The line just barely grazing the top of the two erected walls was used as the 0 reference height. This 0 height was established by sighting across the top of the two walls (sometimes with optical aids) until the center of radiation of the source and the microphone were observed to be exactly on this line. By convention, a source or microphone height lower than this 0 position was called positive (because this was the region that gave increasing attenuation) and heights greater than this 0 position were called negative (because, in general, movement of the source or microphone in this direction reduced the attenuation observed). Note that this is the opposite of a normal up-down/positive-negative convention. For each measurement sequence, the position of the source and the microphone above or below this reference plane was recorded along with the acoustic data. Also measured and recorded were the horizontal spacing between the center of radiation of the microphone and the nearest wall (M), the horizontal distance between the two walls (W), and the distance between the source and the wall nearest to it (S). As in the single wall experiments, the acoustic measurements were conducted at both 5.19 kHz and 10 kHz.

It should be pointed out that there is no reduction in generality caused by keeping the tops of the two walls at the same height above the floor. Having the source and microphone at different heights produces the same effect as having one wall higher than the other. All the following configurations can be simulated:

walls at the same height
walls at different heights
both walls blocking the line of sight
both walls below the line of sight
one wall above the line of sight and one below it.

Table I. Two-wall measurement data for Experiments G1-G13 (5 kHz/10 kHz, in decibels). (See Appendix D for experimental parameters.)

Source (cm)	Mic (cm)	G1	G2	G4	G5	G7A	G8	G9	G9A	G10	G11	G12	G13
0	0	8.6/ 8.6	8.6/ 9.0	7.2/ 7.3	7.4/ 7.2	7.3/ 7.3	10.1/10.5	11.6/12.0	11.2/11.5	7.0/ 7.2	8.0/ 7.9	10.9/10.8	6.4/ 6.4
	.5	8.9/ 9.0	8.8/ 9.1	7.3/ 7.4	7.5/ 7.5	7.5/ 7.5	10.5/10.9	12.3/13.0	11.7/12.2	7.1/ 7.3	8.1/ 8.0	11.3/11.4	6.6/ 6.6
	1						10.7/11.1		12.2/12.6				
	2				7.8/ 7.9	7.5/ 7.6	11.1/11.7	13.5/14.7	13.4/14.3				
	6			8.1/ 8.4		7.6/ 7.7	12.8/13.7	16.8/19.1	16.7/18.8				
	10										9.7/10.1		
	15			9.3/10.0	10.4/12.2		16.3/18.3	22.4/25.9	22.4/25.6				
	20					9.0/ 9.6		23.1/27.4		9.6/10.7	11.1/12.4	21.7/23.9	9.3/ 9.8
	25							25.0/28.6	25.3/28.7				
	30	17.3/19.9	14.1/15.8					26.8/31.2	26.9/31.0				
	40			12.0/13.4	15.5/19.0	10.5/11.6	23.2/26.0	31.9/36.1	31.5/35.5	11.8/13.2		25.7/30.6	10.5/12.1
.5	0		8.5/ 8.6						11.5/12.1	7.2/ 7.4		11.2/10.9	6.4/ 6.7
	.5		8.8/ 9.3	7.4/ 7.6	7.8/ 7.8	7.6/ 7.7	10.7/11.2	12.3/13.2	12.1/12.7				
	6		10.0/10.6										
1	1						11.2/11.8		13.1/14.1				
2	0		9.2/ 9.5						12.7/13.8				
	2		9.7/10.1	8.2/ 8.4	7.9/ 8.6	8.5/ 9.0	11.9/12.6	15.5/17.4	14.6/16.4	7.9/ 8.4		13.1/14.6	7.6/ 7.7
	6		10.4/11.1										
4	4		10.6/11.6										
5	10										10.9/12.1		
	20									11.2/13.5		24.2/28.1	10.2/11.5
6	0								15.5/17.5				
	6			10.1/10.8	9.3/10.4	10.5/11.7	15.6/17.4	22.3/26.6	20.6/24.6	10.0/11.0		18.0/21.3	8.6/ 9.7
10	-10										10.1/10.3		
	- 5									9.4/10.0		13.1/13.3	8.5/ 9.2
	0							21.2/23.1	18.3/20.4		11.6/12.5		
	5										12.0/13.4		
	6								23.4/27.8				
	10										13.1/15.5		
	15								29.2/34.0				
	30									14.0/16.1		30.3/ -	12.0/14.0
15	-40	4.3/ 4.7	6.2/ 5.9										
	-10	12.0/13.6	11.1/12.6										
	0			12.6/13.8	9.8/10.8	14.2/16.7	16.6/18.4		21.5/23.5				
	6							30.0/33.6	26.8/30.7				
	10	17.7/21.3	15.1/17.7										
	15			13.9/16.0	12.8/15.4	15.0/18.1	22.1/26.2	35.9/40.0	32.6/36.9				
	40	24.5/29.5	19.9/24.5	16.0/19.3	17.4/21.5	16.8/20.6	28.9/33.2						
20	-20									15.3/18.5			
	0									12.6/14.4		21.6/23.8	12.0/14.0
	5									13.0/14.8		24.2/28.1	12.5/15.1
	20											32.3/ -	14.2/17.0
25	0								26.1/28.7				
30	10									16.3/18.9		30.7/ -	15.6/18.6
40	-40	12.8/15.4	13.4/14.9										
	-30	14.7/18.4											
	-10	19.5/21.7	17.7/21.1										
	- 6	20.0/21.9											
	0	21.1/23.8		18.4/22.3		22.3/24.8	24.3/26.6		30.3/32.9	16.7/19.5		27.0/28.2	17.1/19.6
	6	23.5/26.0											
	10	25.0/28.9	21.3/26.2										
	15	26.0/30.0		19.2/23.6		22.7/25.4	29.3/33.2						
	20	27.2/31.6											
	25	28.9/33.5											
	30	30.0/34.3											
	35	31.1/36.0											
	40	31.6/35.6	25.2/31.7	21.2/25.9	20.2/23.9	24.5/27.6	33.8/ -						

Table I, cont.

Source (cm)	Mic (cm)	G1	G2	G4	G5	G7A	G8	G9	G10	G11	G12	G13
0	-40			2.7/ 1.5	- .7/- 1.4	4.3/ 3.0	1.3/- .3	2.5/ 1.7				
	-30	.2/- .8	3.2/ 1.7									
	-20					5.9/ 5.3			4.4/ 3.3		3.1/ 3.0	4.1/ 3.2
	-15			5.5/ 4.8	3.8/ 2.9		4.5/ 3.4	4.4/ 4.4				
	- 6			6.6/ 6.1		6.4/ 6.5	7.9/ 7.2	6.3/ 5.5				
	- 2				6.5/ 6.8	6.8/ 6.9	9.4/ 9.5	9.9/ 10.0				
	- .5	8.4/ 8.1	8.3/ 8.5	7.2/ 7.3	7.0/ 6.9	7.0/ 7.0	10.1/ 10.3	11.1/ 11.6	6.5/ 6.9		10.6/ 10.5	6.2/ 6.2
- .5	- 6		7.0/ 7.0									
	- .5		8.1/ 8.3	7.5/ 7.1	6.2/ 6.8	6.7/ 6.8		10.8/ 11.0				
	0		8.4/ 8.4						7.2/ 6.5		10.6/ 10.6	6.4/ 6.7
	.5									8.3/ 8.3		
- 2	- 6		6.6/ 6.1									
	- 2		7.5/ 7.2	6.5/ 6.0	6.1/ 6.4	6.4/ 5.9	8.5/ 8.2	7.5/ 6.5	6.0/ 5.7		8.5/ 7.6	5.8/ 5.3
	0		7.8/ 7.6									
- 4	- 4		6.4/ 5.3									
- 5	5									7.1/ 6.8		
	10								6.6/ 6.4		13.9/ 14.4	6.0/ 6.1
	20									9.2/ 9.9		
- 6	- 6			4.6/ 3.4	4.5/ 4.0	3.7/ 2.5	7.0/ 5.9	.8/- 1.6	4.4/ 4.0		3.8/ 1.7	4.1/ 3.5
-10	-15								1.9/ -		- 1.4/- 1.1	2.0/ .4
	-10									2.7/ 1.1		
	20									7.7/ 8.0		
-15	-40		- 1.4/- 1.4	- .7/- 1.3	- 1.2/- .5	- 1.3/- 1.2	- .7/ 1.3	.3/ .2				
	-30	- 1.5/ 2.0										
	-15			.8/- .8	1.6/ .1	- .3/- 1.3	- .9/- 2.3	.8/- .7				
	-10	- .4/- 1.7	1.9/ .6						.3/- .5	1.6/- .2	- 1.6/- 1.5	1.1/- .5
	0			2.3/ 1.0	4.6/ 3.4	.7/- .7	4.1/ 2.8	4.8/ 4.2		3.0/ 1.5		
	10	5.6/ 5.0	5.1/ 4.5									
	30	11.4/ 12.0										
	40		10.6/ 11.2									
-20	-20								- .6/- 1.5		.4/- .7	- .9/- 1.3
	0								- /- 1.1		2.9/ 3.6	.8/- .5
	20								3.4/ 1.9		13.8/ 17.0	3.2/ 2.0
-30	-30								- 2.7/ -		- .5/ .8	- 1.0/ 1.6
-40	-40	- .3/ .1	.4/ .4	- /- .5	- / .3	- - / .1	- .2/ .1					
	-15			- .7/- .1	- 1.1/- 1.4	.8/ .4	- .9/ 1.1	.3/ .4				
	-10	- .2/ .6	- .9/- .8									
	0			- 1.6/- .7	.7/- .7	.7/- .2	1.0/- .1					
	10	.2/- 1.0	.3/ -									
	40	7.6/ 8.5	5.3/ 5.6									

DEVELOPING THE ALGORITHM

Guiding Principles

First of all, we were seeking a generalized calculating procedure that would hold for any frequency and for any geometry, or at least for all of those of interest in the design of highway noise barriers. To facilitate testing a proposed algorithm's ability to encompass wavelength changes, it was therefore very important that the measurements take place at at least two frequencies separated by an octave or more (in this case, 5.19 and 10 kHz) to allow definitive tests where only the wavelength was changed and not the geometric properties. In addition, it was very important to formulate any possible algorithms so that in principle they would hold for a wide range of frequencies. This means that the equations should be formulated so that either (1) the frequency-dependent terms cancel out dimensionally and remain merely as ratios, or (2) the frequency is combined with appropriate distance terms which are then described in terms of wavelengths rather than absolute dimensions.

Steps in the Development

Finding algorithms that matched the experimental results better than the leaning pole theory was not particularly difficult, since the leaning pole theory did so poorly; however, finding algorithms that would predict reasonably close to the actual experimental data proved very time consuming and difficult. Many possible algorithms were proposed. Each, in turn, was subjected to correlation with the experimental data. Next, their possible areas of weakness were considered and additional experiments were conducted to explore an increasingly full range of possible geometries. Frequently, an algorithm would be found that would explain the experimental data to date, but when subjected to other geometries would be found less appropriate. In that case, either the algorithm was refined or a new concept was instituted. Among other things, we tried to find a single equivalent wall theory (improvement of the leaning pole theory); we also tried manipulations of the Fresnel numbers as well as manipulations of the attenuations. This report makes no attempt to discuss all of these schemes in detail. The purpose of this section is to outline the general nature of the pursuit, and thus help the reader understand how the final algorithm was derived and why it was chosen.

The initial geometries were picked to represent the middle of the range most likely to be encountered in highway design problems. Thus the source and microphone were typically separated by 400 cm (scaled to highway frequencies, this would be equivalent to about 80 m (260 ft) between the car and the listener) with a distance of 120 cm between the

source and the first wall and with a separation between walls of perhaps 140 cm. For this configuration, it was found that the results of the actual two-wall acoustic measurements could be "predicted" by the use of a relatively simple algorithm, namely,

$$R = A + 0.5\ B\ ,$$

where

R = the resultant attenuation of the two walls, in decibels

A = the attenuation of the more attenuative of the two walls when considered alone, in decibels

B = the attenuation of the less attenuative of the two walls when considered alone, in decibels.

This formula held for the range of relative heights of the source and the microphone tested to that time--both the source and the microphone could be in any position from 60 cm below the line of sight to just above the line of sight. Calculations based on the above formula gave rather good predictions; furthermore, it worked equally well at 5 or 10 kHz.

At this juncture, the predictive capabilities of this relatively simple formula looked very good. However, when the wall spacing was varied, it was found that the number it was necessary to multiply the less attenuative wall by was no longer always 0.5, but rather varied from 0 up to 0.6 depending on the geometry involved. Figure 9 shows the results of hundreds of individual measurements where the horizontal distance between the source and the microphone was held constant at 394.5 cm and the distance between the source and the nearest wall was fixed at 121.5 cm, but the spacing between the walls was varied from 0 to 180 cm. In the figure, K represents the decimal fraction that the attenuation of the less attenuative wall (in decibels) must be multiplied by before being added to that of the other wall; i.e.,

$$R = A + KB.$$

It was found that for each wall spacing there was a particular value of K that would predict the actual experimental results quite closely. (Note, for example, the K of approximately 0.5 for the 140 cm spacing of the initial experiments.) The value of K goes to 0 if the wall spacing goes to 0; this agrees with theoretical considerations, since the algorithm must reduce to the single wall calculation under this condition. For even wider spacings than shown on the plot, the value of K tends to settle out at about 0.6.

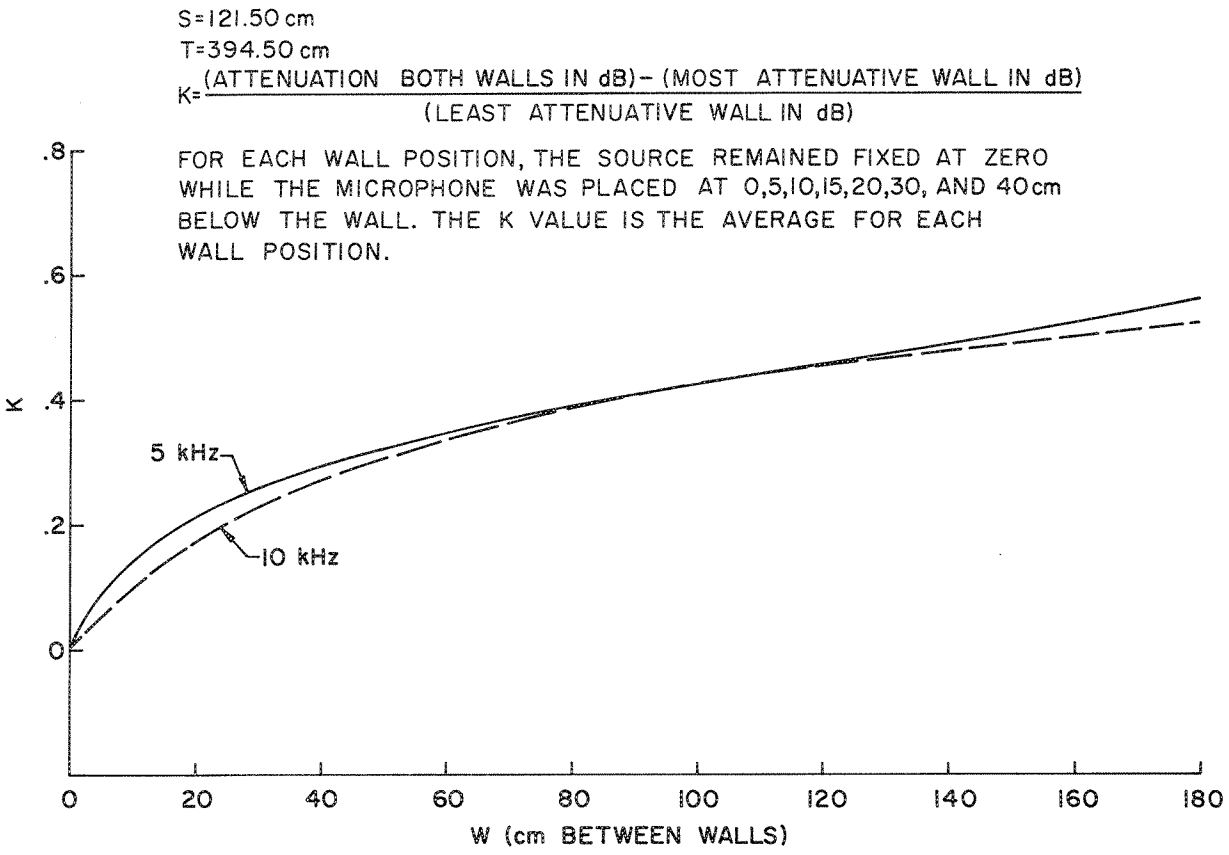

Figure 9. K vs wall spacing (in cm).

One very important characteristic of this curve was that the value of K required for a given wall spacing was substantially the same at both 5 and 10 kHz. This was, at the time, very puzzling because the physical phenomena would suggest that the spacing of the walls in wavelengths (which, for a fixed geometry, would give a frequency-dependent effect) would be an important parameter in the computation. Figure 10 is essentially the same as Figure 9 except that the spacing between walls has been expressed in wavelengths rather than a linear dimension. As can be seen, the resulting K values are different at 5 kHz and 10 kHz whereas in the previous figure they were independent of frequency. This was just the opposite of what might have been expected, and strongly indicated that the wall spacing expressed in wavelengths was not one of the primary parameters needed for predicting the two-wall case.

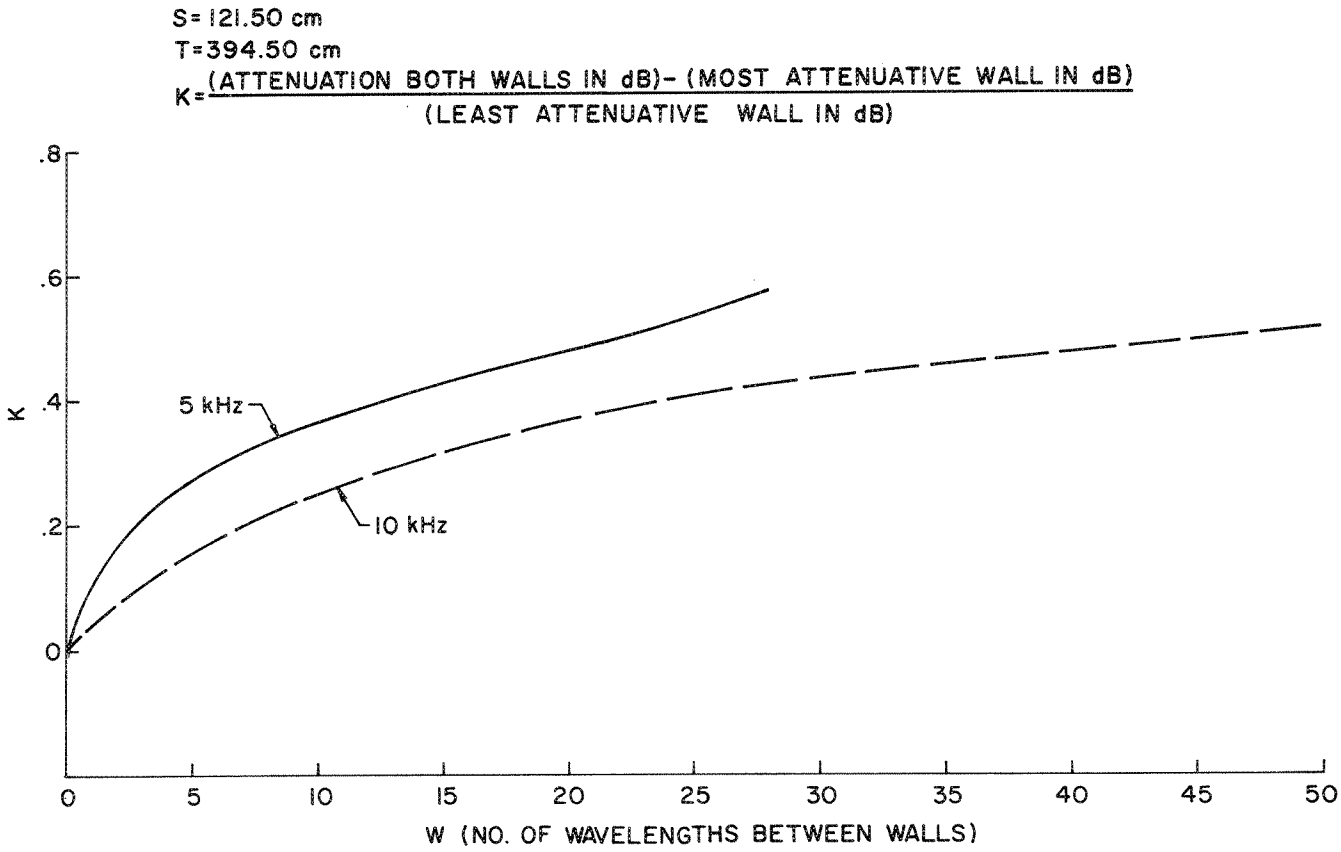

Figure 10. K vs wall spacing (in wavelengths).

A naive interpretation of the results would indicate that the two-wall effect was functionally dependent on the wall spacing when measured in centimeters. This was, of course, a totally unacceptable supposition since it would leave a solution that could not be scaled to other frequencies; i.e., a direct measurement in centimeters would not fulfill the basic requirement that the geometric measurements used for computation must ultimately be either in wavelengths or in dimensionless ratios.

Since the experimental results refuted the notion that the wall spacing in wavelengths was a primary factor, we began searching for appropriate geometric ratios that might prove useful in predicting the results of the experimental measurements. Many proposed geometric ratios were investigated, involving much calculation and the experimental determination of many additional hundreds of individual data points.

The result of these investigations indicated that one of the primary ratios involved was W/T, the horizontal distance between the walls divided by the horizontal distance between the microphone and the receiver. In other words, a primary geometric property was the percentage of the total distance between the source and the receiver occupied by the space between the walls.

To determine that it was indeed the W/T ratio that was important, and not phenomena involving the individual distances between the source and the first wall (S) and the microphone and the last wall (M), two types of experiments were carried out. In the first, the total distance between the source and the microphone was held constant as was the spacing between the walls, but the position of the two-wall system between the source and the microphone was varied. This varied the values of S and M, but left the W/T ratio unchanged. This procedure did not essentially alter the results. In the second experiment, all the geometric ratios were maintained, including the W/T ratio, but the overall scale was expanded and contracted. Again, the results remained unchanged. (These effects are examined in the context of the "final" algorithm on p.18).

The majority of the data used to compile the figures showing that the K value was constant for any given fixed horizontal spacing was, however, taken from configurations where both walls were reasonably attenuative when considered individually. When the possible formula was examined with regard to its ability to predict a wider range of configurations, particularly where one or both walls were not blocking the line of sight, it was found wanting. In addition, although the calculation was simple, and effective for those cases where it applied, it did not conform to a good conceptual model in that it did not seem indicative of what was physically taking place. Therefore the approach was abandoned.

Development of the Final Algorithm

Conceptually, the sound could be considered to go from the source to the top of the first wall, and to reradiate from there (Huygens' principle) back down to the receiver, passing the second wall in the process. An actual numerical integration of Huygens' principle for the reradiation above the first wall would be complicated and would probably have to be repeated on a case by case basis rather than yielding a general formula. We therefore decided to try a very simplified approach using the Huygens concept as a philosophical guide; this involved substituting an imaginary point source for the Huygens numerical integration process. More specifically we calculated the attenuation produced by the more attenuative wall and then added to it the attenuation that would be produced by a second wall for a new point source located atop the first wall. To find the more attenuative wall, we first computed

two N values used with ordinary Fresnel curves for calculating diffraction. The geometry involved is shown in Figure 11. As can be seen, the N value for the first wall was computed as though no other wall were in existence; the resulting attenuation, in decibels, was then obtained by referring to Fresnel's curves (see Appendix A). In a similar fashion, the attenuation of the second wall was found. Whichever wall was the more attenuative then became the "main" or "first"* wall, and the attenuation calculated for it (in decibels) was given the label F. Next, a new radiation source was assumed to exist at the top of this wall and an N value was computed for the path from this source to the receiver, as shown by the dashed lines in the bottom diagram of Figure 11. The N value calculated from this geometry was then applied to Fresnel's diffraction curves and the resulting value, in decibels, was given the label J.

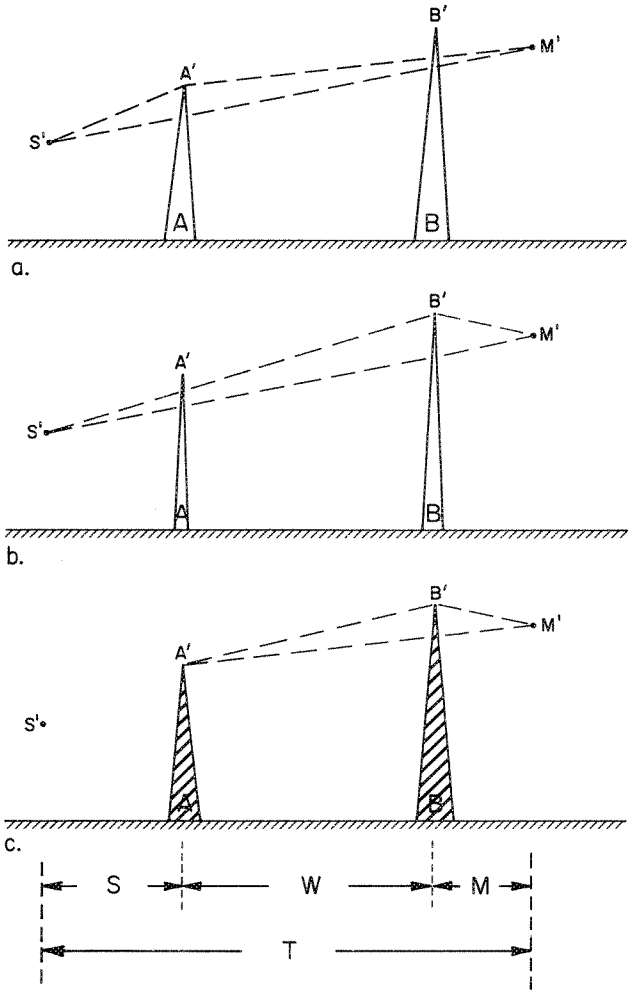

Figure 11. F and J calculation geometry.

*It does not matter whether this "first" wall is nearer the source or nearer the receiver since it can be assumed that reciprocity applies.

As a first approximation, the total attenuation (in decibels) of the two walls taken together was assumed to be F+J. In Figures 12, 13, and 14, the experimental attenuations for a wide range of two-wall geometries (the ordinate) are plotted against the values of F+J calculated for the geometries involved in each data point. If F+J exactly predicted the experimental result, the resultant "curve" would be a series of dots all falling on a straight line at a 45° angle from the origin. This is substantially true for large W/T ratios as shown in Figure 12 where one wall is quite near the source and the other wall is quite near the receiver and there is a relatively wide spacing between walls. Smaller W/T ratios tend to form parallel lines below the 45° slope, indicating that, in these cases, F+J predicts too much attenuation as can be seen from Figures 13 and 14.

Obviously, the correct algorithm had to contain terms or factors that were a function of W/T. The fact that the lines in Figures 12, 13, and 14 appeared in parallel indicated that this correction must be in the form of an additional term to F+J rather than a factor; this term must be a function of W/T and would carry a negative sign (to correct for the over prediction).

Figure 13 shows the values obtained when the total distance between the source and microphone remained fixed at 769.80 cm and the spacing between the walls remained fixed at 28.40 cm, but the position of the two-wall system relative to the source and microphone was varied. As can be seen, the data all tend to fall on the same line, indicating that it is the W/T ratio that matters in evaluating the correction term and not the other horizontal dimensions. This conclusion was strengthened by the data presented in Figure 14, which shows the results when the W/T ratio was held constant at 0.242 but the scale was changed by varying W and T proportionately. Once again, the data all tend to fall on the same line.

Because the data deviated from parallel lines for lower values of attenuation (roughly, below 10 dB) and tended to fall more toward 0, the corrective term to be subtracted from F+J also had to be functionally related to the value of F or J, or perhaps both. Our original assumption was that it was a function of the sum of F+J. This worked for a medium range of attenuative values; however, it tended to break down at very low values of J. It was finally decided that the effect was due primarily to the fact that J itself was reducing to 0 and that much better results would be obtained by attaching the functional dependence to J alone rather than to F+J. The functional dependence on J had to be such that for large and small values of J the dependence disappeared; that is, for large values of J, the function of J in the corrective term must approach unity, and for small values of J it must approach 0. It was found (as will be explained later) that the J dependence of the correctional term should take the form

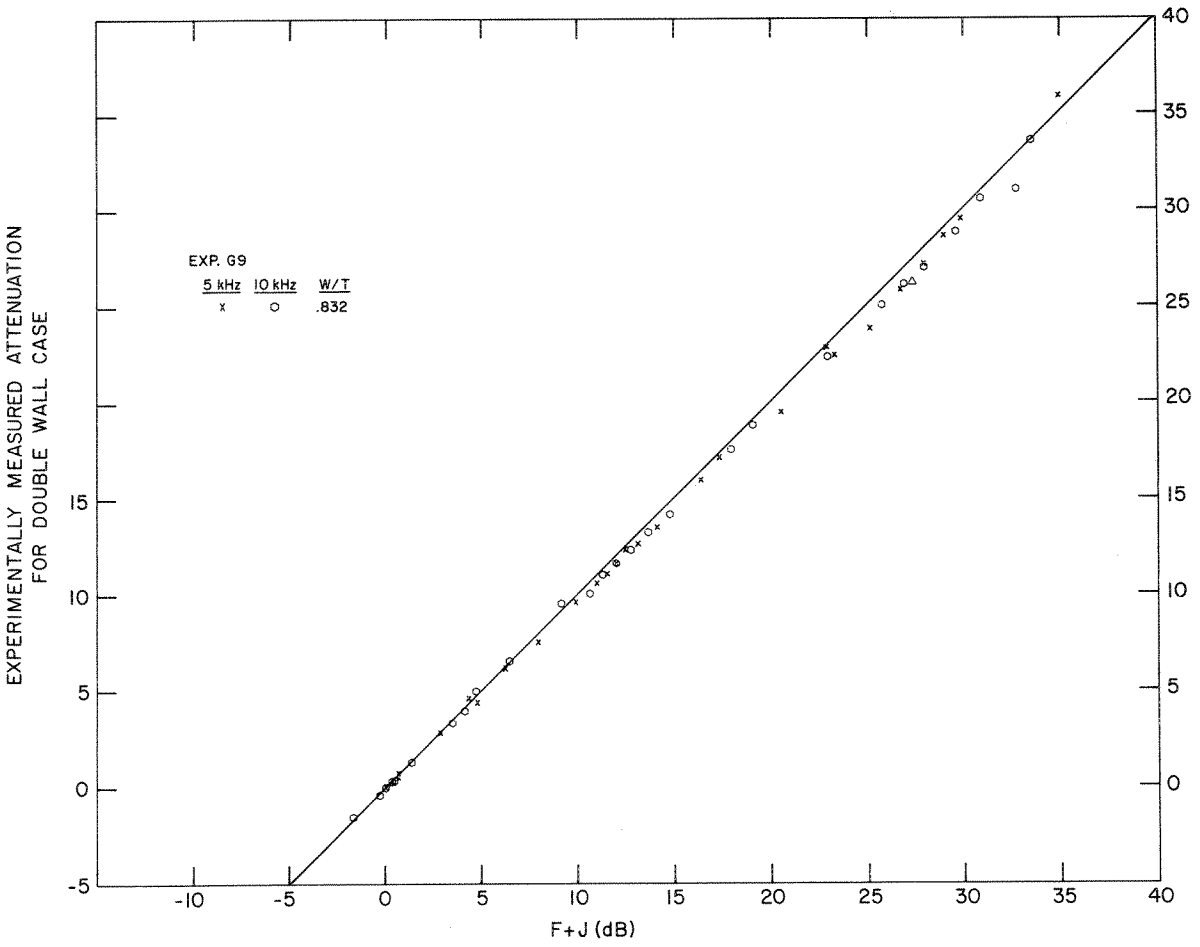

Figure 12. Experimental attenuation vs F + J for large W/T ratio.

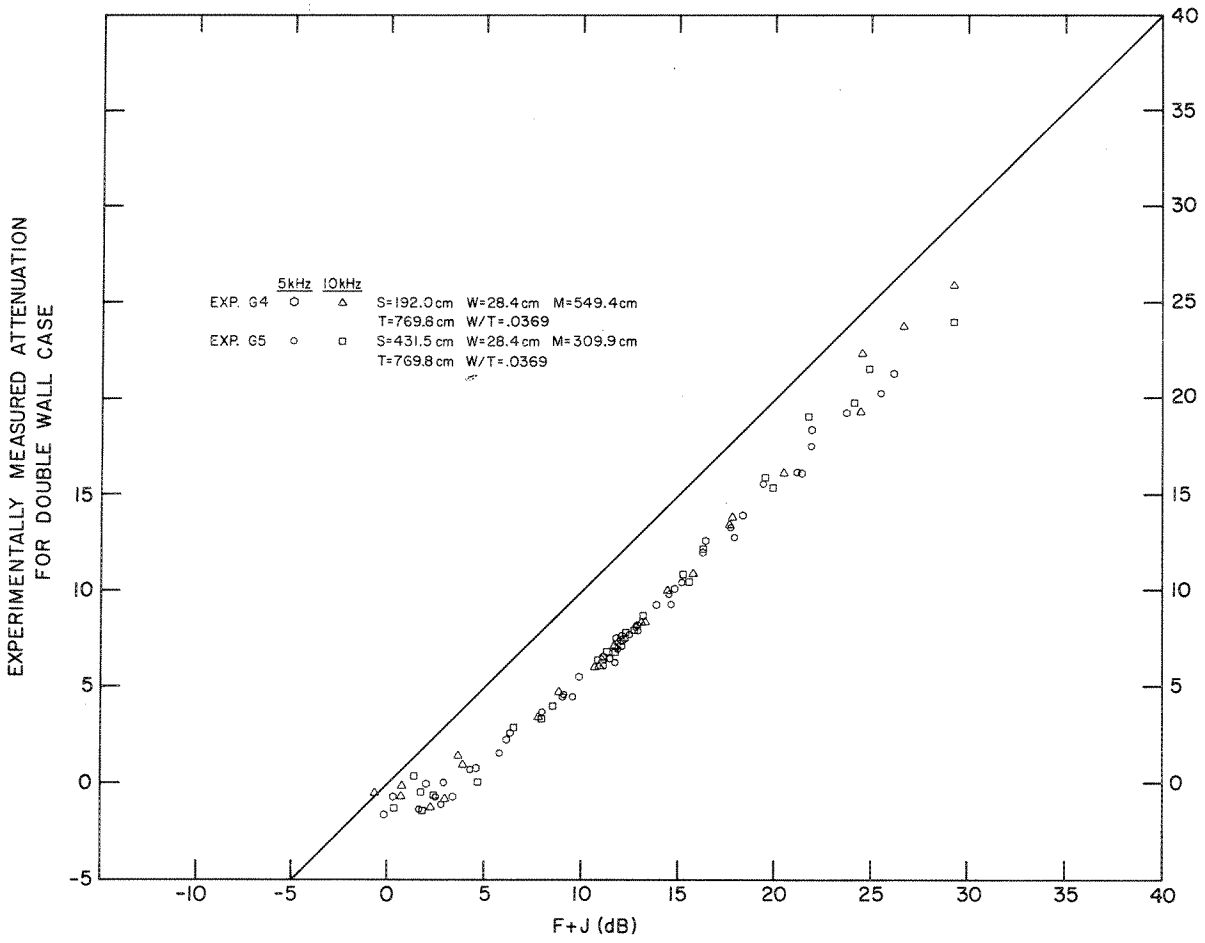

Figure 13. Experimental attenuation vs F + J for small W/T ratio.

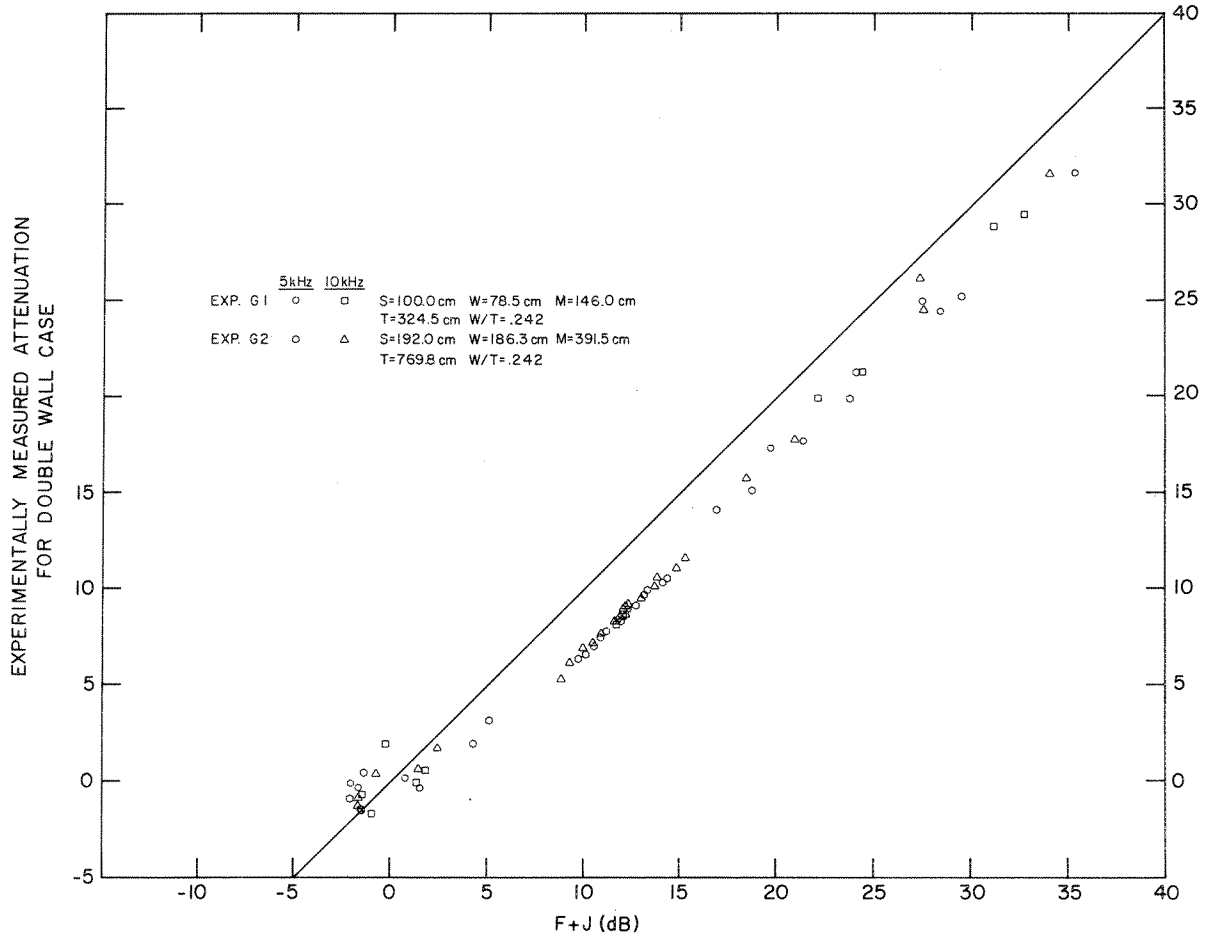

Figure 14. Experimental attenuation vs F + J for medium W/T ratio.

$$1 - e^{-J/2} .$$

The other major functional dependence of the corrective term concerned W/T. Although the lines for different W/T ratios in Figures 12-14 were all parallel, the spacing between these lines was obviously not linearly dependent on W/T. W/T ratios over about 0.8 tended to be very close to the line through the origin whereas W/T ratios below a few tenths tended to lie about 6 dB away.

To find out the nature of the dependence on W/T, we took the data for each particular W/T ratio; for each data point of this ensemble, we then calculated F (the attenuation of the more attenuative wall when considered by itself) and added to this J (the attenuation due to a second wall placed between the receiver and a source located on the top of the first wall) and subtracted from this sum the measured experimental value for that data point. This value (in decibels) was the total corrective term needed to make the calculation exactly predict the results of the experiment for that particular data point. For some of the data points, the J function was such that part of of this correction was already being taken care of by the factor $(1-e^{-J/2})$. To find the amount of correction that the W/T term alone would be required to make, we divided the results of (F+J - experimental values, in decibels) by the factor determined from $(1-e^{-J/2})$. The net result was the number of decibels, due to W/T alone, that would be required in the correction term to make the calculation precisely match the experimentally measured attenuation for that particular data point at that W/T ratio. This process was repeated for all of the data points for a given W/T ratio where J = 2 dB or more; i.e., where J was large enough that the J function itself was not the primary determinant of the size of the corrective term. The mean and standard deviation of this list of correctional requirements (in decibels) were then obtained for this particular W/T ratio. These values for one W/T ratio are represented by one data point on the plot shown in Figure 15; the mean value is shown as the dot and the extent of the line with the bars on the end encompasses plus or minus one standard deviation. This entire process was repeated, in turn, for a range of W/T ratios, as displayed in Figure 15. The functional relationship chosen for use in the final equation to produce the required correction is plotted as a solid line in the figure. The correction calculation was chosen for simplicity of implementation on a computer or calculator in that it does not have a bounded range of applicability. The resulting W/T dependence that was incorporated in the correction term was as follows:

$$6\, e^{-(3/2)(W/T)} + 1.3\,(e^{-35W/T} - 1) .$$

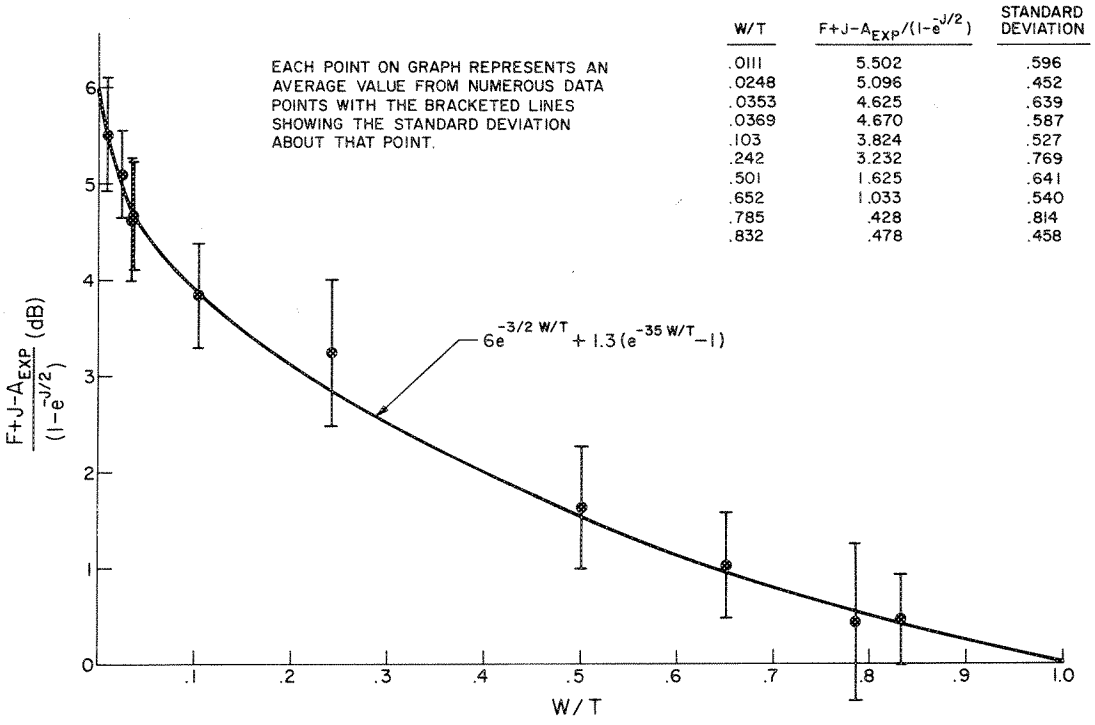

Figure 15. Correctional factor due to W/T alone.

Using this term, we tried the same procedure as a check on the term $(1-e^{-J/2})$. By subtracting the experimental values, in decibels, from F+J and dividing the results by the W/T correctional term just given, we found the additional correction factor due to J alone. The results are shown in Figure 16. As can be seen, there appears to be some spreading in the data. However, considering the scale of the graph and the fact that it contains all the residual experimental error, $(1-e^{-J/2})$ appeared to be more than acceptable.

The final result was

$$ATTN = F+J - \left[6\,e^{-(3/2)(W/T)} + 1.3\,(e^{-35W/T} - 1)\right](1 - e^{-J/2}) .$$

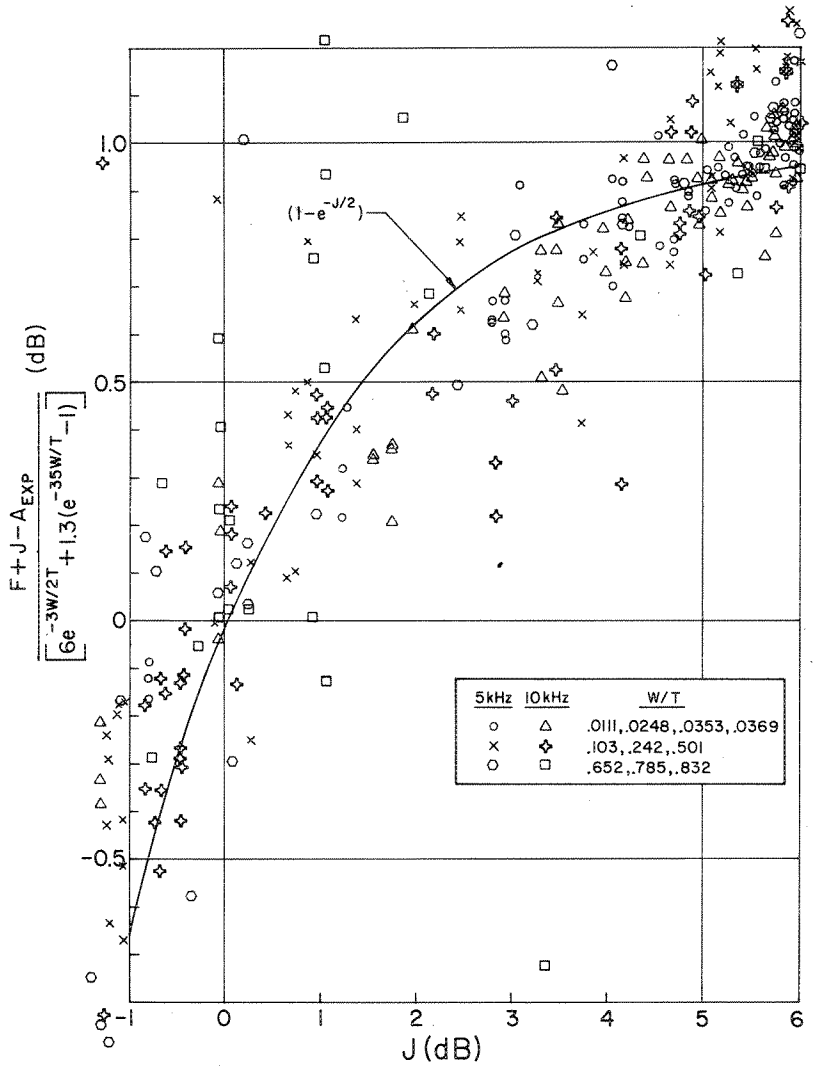

Figure 16. Correctional factor due to J alone.

RESULTS

Figure 17 covers a very wide range of data points where the experimentally measured values for the two-wall case are plotted against the attenuation that was calculated from that geometry using the foregoing equation.

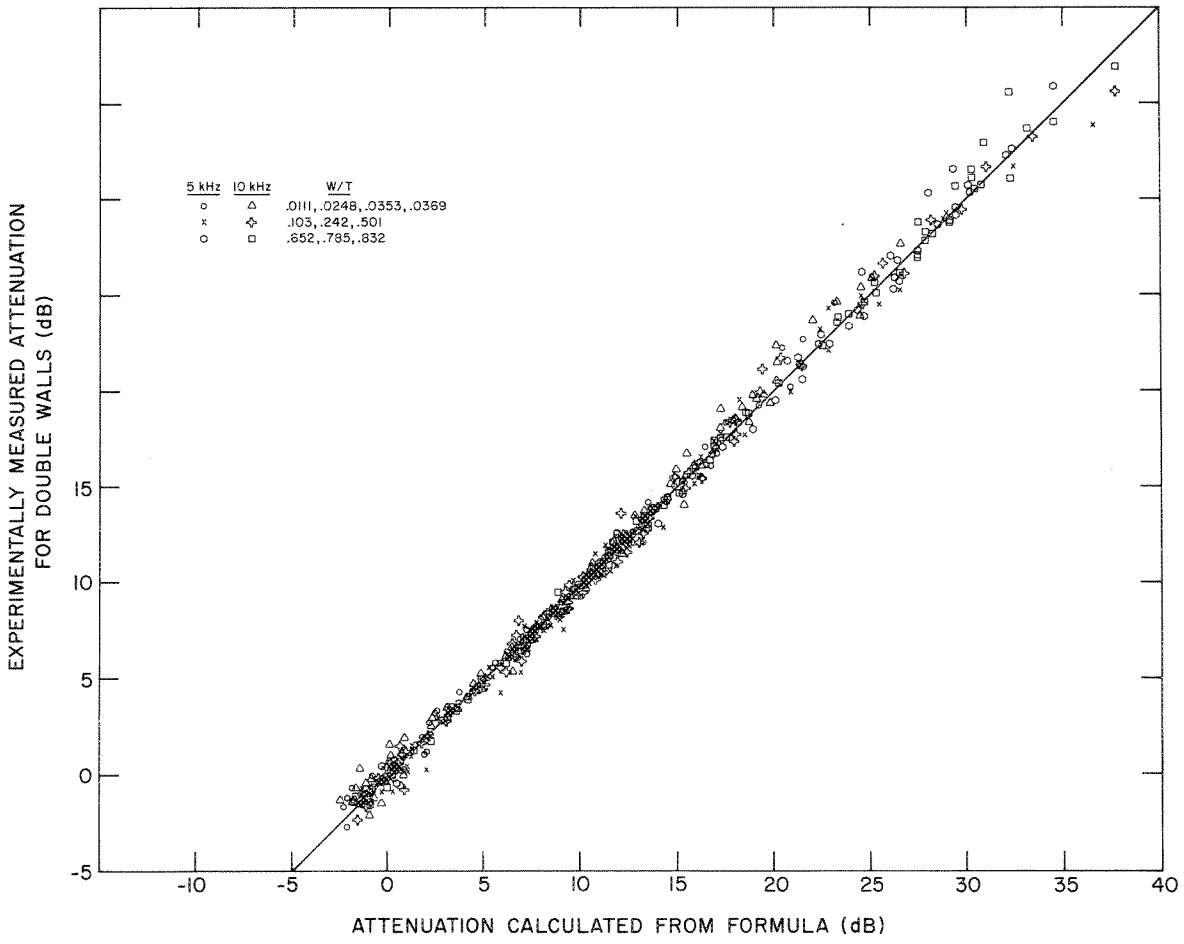

Figure 17. Experimental attenuation vs calculated attenuation using final algorithm.

As can be seen, the data form a "line" remarkably close to 45° through the origin. The predictive capability of the equation is good when both walls are high (the slightly greater scatter of points above 30 dB is believed to be caused by experimental measurement problems rather than by any deficiency in the formula). It is good when both walls are near a grazing line of sight, in which case the attenuation ranges from 6 to 12 dB depending on the W/T ratio, with large W/T ratios giving the larger attenuation. It is still good when the noise source and the receiver are both so far above the walls that the attenuation approaches 0. The equation even works reasonably well when the walls are situated in positions below the source and the microphone such that the signal is enhanced rather than attenuated.

USING THE FORMULA

The formula developed as a result of this study accurately predicts the diffraction caused by two cascaded barriers or screens and can be applied to a wide variety of cases, including all geometries of interest in highway noise suppression design. Note that the formula is for point sources, and is for diffraction only; i.e., it does not include terms for spreading loss or other attenuation.

The formula is

$$D = F + J - \left[\left[6\, e^{-\frac{3W}{2T}} + 1.3\left(e^{-\frac{35W}{T}} - 1\right)\right]\left(1 - e^{-\frac{J}{2}}\right)\right],$$

where

D = the total attenuation, in decibels, created by the presence of the two walls.

F = the attenuation, in decibels, that would be produced by the more attenuative of the two walls when considered singly (as though the other wall were not there).

J = the attenuation that would be produced by the remaining wall, assuming a new radiator now exists at the top of the more attenuative wall (i.e., the effect of the remaining wall on the sound from this new source).

$\frac{W}{T}$ = the ratio of the horizontal spacing between the two walls (W) to the total horizontal distance from the source to the receiver (T).

The use of the formula can perhaps be made clearer by referring to diagrams a, b and c in Figure 11. In these diagrams, there is a source located at S′, and a listener or microphone located at M′; between them are two walls, one labeled A and the other, B. The dashed lines in Figure 11a show the geometry involved in calculating the attenuation that would be created by wall A if wall B did not exist. Briefly, this calculation consists of obtaining the direct distance between S′ and M′ and then taking the difference between this value and the sum of the two straight paths that the shortest sound ray would actually have to follow; namely, from S′ to A′, and from A′ to M′. This path length difference, δ, is then used to find the Fresnel number N:

$$N = \frac{2\delta}{\lambda},$$

where

λ = the wavelength of the radiation in question.

Fresnel's curves are then consulted using this N to compute the amount of attenuation, in decibels, that wall A would create by itself. (For a detailed explanation of the calculation of the Fresnel number N and the use of Fresnel's equations, see Appendices A and B.) A similar procedure is followed to calculate the diffraction that would be caused by wall B if wall A did not exist, using the geometry shown in Figure 11b.

These two attenuations are then compared and the one that is the greater becomes term F of the equation. If they are nearly equal, it does not matter which one is chosen. For the purpose of illustration, we are assuming that wall A has the greater attenuation.*

We now compute the J term in the equation; this is the attenuation, in decibels, that would be created by wall B for a "new" sound source located at the top of wall A. This calculation is accomplished using the geometry shown in Figure 11c.

For those cases where $W/T \to 1$ (i.e., where the source is near one wall and the microphone is near the other wall and the walls themselves are widely separated), the correct value for the two walls is very nearly the sum of F+J directly. For other configurations where W/T does not approach unity, the sum of F+J will, by itself, predict too much attenuation by up to 6 dB. The function of the complicated third term in the equation is to correct for this and allow accurate predictions for a wide variety of cases. This corrective term can assume values between 0 and 6 dB. It will tend toward 0 if W/T is very large (or if J is very small); on the other hand, if W/T is fairly small, the corrective term will tend to approach 6 dB.

Note that if the two walls are of equal height and so close together that they almost merge into one, the formula degenerates to D=F (as it

*It really doesn't matter whether the more attenuative wall is nearer the source or the receiver since it can be logically assumed that reciprocity applies, and that, as far as the overall transmission loss is concerned, the results would be the same if the source and microphone were interchanged in position. It is conceptually somewhat easier to think of the more attenuative wall (probably in most cases meaning the higher wall) as being that closer to the source.

should) because J would be 6 dB* and the correction term would be -6 dB (because of the very small W/T ratio), and they will thus cancel each other out, leaving D=F. Another circumstance that should reduce to the single wall case is when one wall is so much below the other that the computation for J will yield no attenuation, i.e., when J=0. Because both the J term itself and the corrective term will be 0, the formula once again reverts to D=F (as it should).

For cases in between, it was experimentally found that this formula very closely predicts the attenuation for a wide variety of experimental situations. Figure 17 shows the experimental values obtained from a wide variety of two-wall cases plotted against the values predicted by the formula from the geometry of each case. If the experimental error were zero and the formula perfect, these values would fall precisely on a 45° line through the origin. There is actually some small scatter in the data, but the formula predictions and the experimental data come impressively close to this 45° slope.

As can be seen from the attenuation values below 6 to 12 dB in Figure 17, the formula also works well when the wall does not block the line of sight. In this document, this configuration is referred to, by convention, as negative N. For N's down to minus 0.3, the formula can be used directly. For more negative N's, there are certain precautions that should be followed in the use of the formula, since in this region the signal may be enhanced as well as attenuated, depending on the actual value of N:

(1) If N is such as to yield enhancement, the value used for this enhancement in the equation should be a negative number. For example when calculating J, if N were minus 0.7, which would yield an enhancement of about 1.4 dB, this value would appear in the equation as -1.4.

(2) In picking the wall to use for computing F, use that wall which (when considered by itself) has the greatest N in an algebraic not an absolute sense; this, of course, will be the same as the more attenuative wall if both N's are above minus 0.3.

Example Calculation:

An example calculation will now be given for the wall positions and topography shown in Figure 18. Also shown are the necessary parameters.

---

* Wall B would, of necessity, be very close to the grazing line of sight from the top of wall A to the microphone, and all such line-of-sight cases yield an attenuation of 6 dB, regardless of the frequency involved.

Cross Section of Geometry

Source at 566 Hz, 4 ft off the lane center line
Listener's ear 5 ft above ground (λ = 2 ft
Both walls 6 ft high ($\therefore h = \Delta$, in feet)

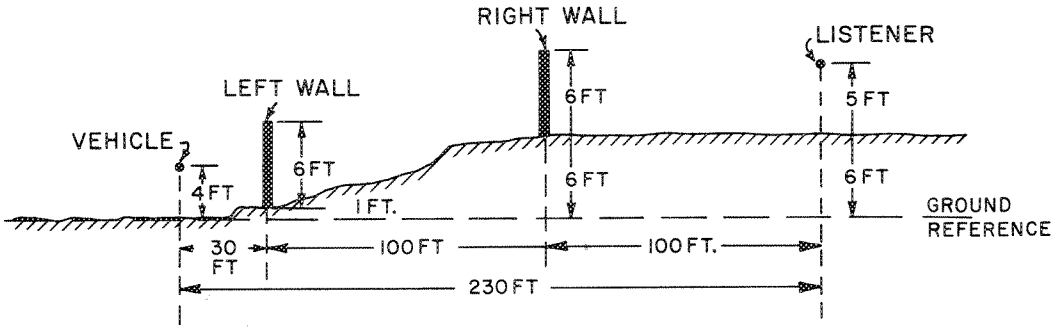

Equivalent geometry with necessary parameters besides λ = 2 ft

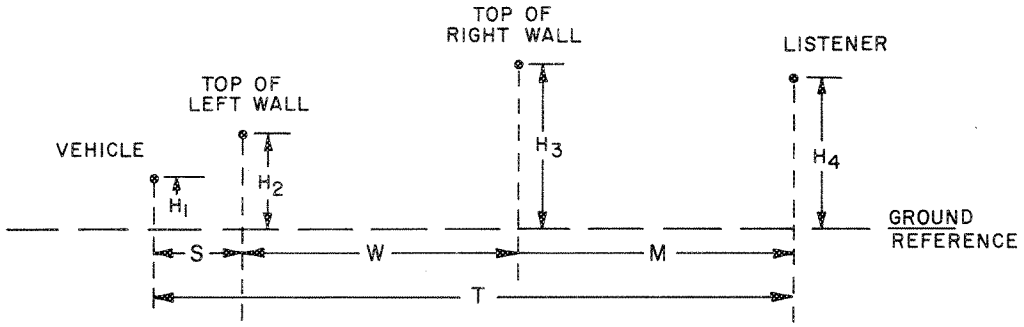

S = 30 ft [horizontal distance from source to first (left) wall along reference line]

W = 100 ft [horizontal distance between walls along reference line]

M = 100 ft [horizontal distance from second (right) wall to listener along reference line]

T = 230 ft [horizontal distance between vehicle and listener along reference line]

H_1 = 4 ft [vertical height of vehicle center above reference line]

H_2 = 7 ft [vertical height of left wall top above reference line]

H_3 = 12 ft [vertical height of right wall top above reference line]

H_4 = 11 ft [vertical height of listener's ear above reference line]

Figure 18. Wall positions and topography for sample calculation.

Step 1. Calculate Fresnel's number N* for each wall

(a) Left wall

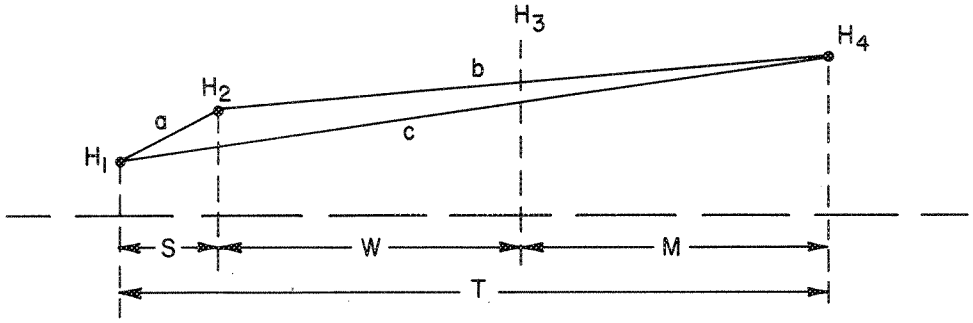

Path length difference $\delta = a+b-c$, where

$$a = \sqrt{(H_2-H_1)^2 + S^2}$$

$$b = \sqrt{(H_4-H_2)^2 + (W+M)^2}$$

$$c = \sqrt{(H_4-H_1)^2 + T^2}$$

Using the appropriate values, we get

$$\delta = \sqrt{(3)^2 + (30)^2} + \sqrt{(4)^2 + (200)^2} - \sqrt{(7)^2 + (230)^2}$$

$$= 30.150 + 200.040 - 230.106$$

$$= 0.084 \text{ ft.}$$

From Appendix A, we find $N = 2\delta/\lambda$. Therefore,

$$N_L = \frac{2(0.084 \text{ ft})}{2 \text{ ft}} = 0.084 .$$ ←

left wall

*See Appendix A for explanation of Fresnel's number N.

(b) right wall

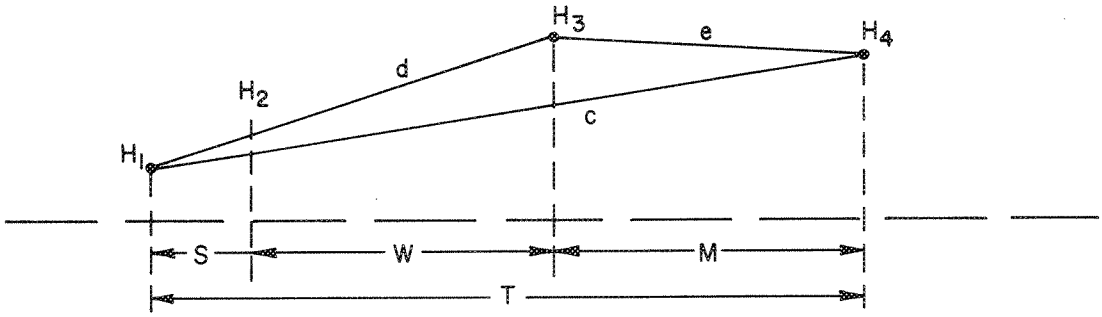

Path length difference $\delta = d + e - c$, where

$$d = \sqrt{(H_3-H_1)^2 + (S+W)^2}$$

$$e = \sqrt{(H_3-H_4)^2 + M^2}$$

$$c = \sqrt{(H_4-H_1)^2 + T^2}$$

Using the appropriate values, we get

$$\delta = \sqrt{(8)^2 + (130)^2} + \sqrt{(1)^2 + (100)^2} - \sqrt{(7)^2 + (230)^2}$$

$$= 130.246 + 100.005 - 230.106$$

$$= 0.145 \text{ ft.}$$

$$N_R = \frac{2(0.145 \text{ ft})}{2 \text{ ft}} = 0.145$$

right wall

Step 2. Choose largest N (the N that gives the most attenuation). Calculate this attenuation and label this value F.

Clearly, $N_R > N_L$, so referring to Appendix B on the use of Fresnel's curves we find

$$F = 5.8 + 10.4\ (0.145)^{0.41} = 10.51 \text{ dB}$$

(N_R)

Step 3. Assume point source at top of the more attenuative wall and calculate new N_J for remaining wall.

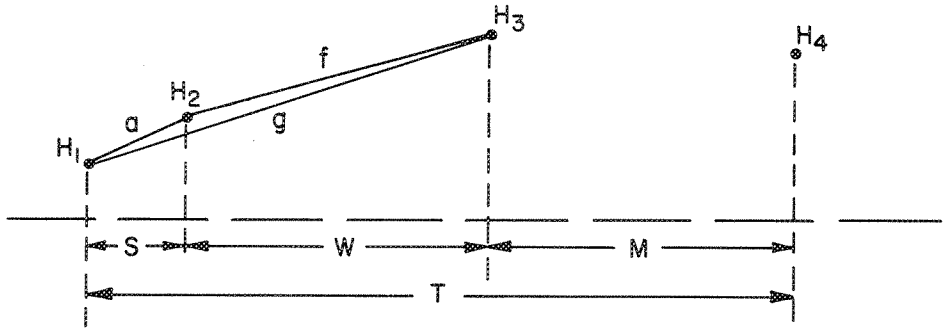

Steps 1 and 2 showed the more attenuative wall to be the right wall; therefore we assume a point source at its top, and calculate a new Fresnel number labeled N_J between this point, the top of the remaining wall, and, in this case, the vehicle at H_1 as shown.

Path length difference $\delta = a+f-g$, where

$$a = \sqrt{(H_2-H_1)^2 + S^2}$$

$$f = \sqrt{(H_3-H_2)^2 + W^2}$$

$$g = \sqrt{(H_3-H_1)^2 + (S+W)^2}$$

Using the appropriate values we get

$$\delta = \sqrt{(3)^2 + (30)^2} + \sqrt{(5)^2 + (100)^2} - \sqrt{(8)^2 + (130)^2}$$

$$= 30.150 + 100.125 - 130.246$$

$$= 0.029 \text{ ft.}$$

$$N_J = \frac{2(0.029 \text{ ft})}{2 \text{ ft}} = 0.029$$

*If the left wall had been the more attenuative, the point source would be assumed to lie on the left wall top, and N_J would be calculated between this point, the top of the right wall, and the listener at H_4.

Step 4. Calculate attenuation from N_J and label this value J.

From Appendix B,

$$J = 5.8 + 10.4\,(0.029)^{0.41} = 8.24 \text{ dB}.$$

(N_J = S)

Step 5. Use the overall formula to calculate total two-wall attenuation.

We have found

$$F = 10.51 \text{ dB}$$
$$J = 8.24 \text{ dB}$$

and we can calculate

$$\frac{W}{T} = \frac{100 \text{ ft}}{230 \text{ ft}} = 0.435.$$

Using the formula,

$$\text{Total Attenuation} = F + J - \left[6\,e^{-\frac{3W}{2T}} + 1.3\left(e^{-\frac{35W}{T}} - 1\right)\right]\left[\left(1 - e^{-\frac{J}{2}}\right)\right]$$

$$= 10.51 \text{ dB} + 8.24 \text{ dB} - \left[6\,e^{-\frac{3}{2}(0.435)} + 1.3\left(e^{-35(0.435)} - 1\right)\right]\left[\left(1 - e^{-\frac{8.24}{2}}\right)\right]$$

$$= \underline{\underline{16.96 \text{ dB}}}.$$

BIBLIOGRAPHY

Fehr, R.O.; "The Reduction of Industrial Machine Noise." Proc. 2nd Ann. Noise Abatement Symp., Armour Res. Found., Chicago: pp. 93-103 (1951)

Jonasson, H.G.; "Diffraction by Wedges of Finite Acoustic Impedance with Application to Depressed Roads." J. Sound & Vibra., pp. 557-585 (1972)

Kurze, N.J. and G.S. Anderson; "Sound Attenuation by Barriers." Appl. Acoustics, V4, #1 - pp. 35-53 (1971)

Maekawa, Z.; "Noise Reduction by Screens." Applied Acoustics, V1, pp. 157-173 (1968)

Pierce, A.D.; "Diffraction of Sound Around Corners and Over Wide Barriers." J. Acoust. Soc. Amer., V55, #5 - pp. 941-955 (1974)

Redfearn, S.W.; "Some Acoustical Source-Observer Problems." Philosop. Mag., V7, #30 - pp. 223-236 (1940)

Seckler, B.D. and J.B. Keller; "Geometrical Theory of Diffraction in Inhomogeneous Media." J. Acoust. Soc. Am., V31, #2 - pp. 192-205 (1959)

Seckler, B.D. and J.B. Keller; "Asymptotic Theory of Diffraction in Inhomogeneous Media," J. Acoust. Soc. Am., V31, #2 - pp. 206-216 (1959)

APPENDIX A

CALCULATION OF THE FRESNEL NUMBER N

In this report, attenuation is calculated though the use of the Fresnel number N. The methods for calculating N for each individual wall (in order to find F) and for the less attenuative wall in relation to the new radiating source (in order to find J) are reviewed below. In all cases, the basic single-wall N calculation is used.

N is a geometrically derived number defined as

$$N = \frac{2\delta}{\lambda}^{*},$$

where

δ = the difference between the geometrical distance from the source to the microphone and the shortest path from the source to the top of the wall and then to the microphone. Referring to Figure A-1, δ = (line segment source-to-wall) + (line segment wall-to-microphone) - (line segment source-to-microphone). Referring to Figure A-2, δ = (line segment source-to-microphone) - (line segment source-to-wall) - (line segment wall-to-microphone).

λ = the wavelength of the sound in the medium of propagation (air in this case) for the frequency used. $\lambda = c/f$, where c is the sound velocity (about 343 m/sec for air at ordinary temperatures) and f is the frequency of the sound in cycles per second (Hz).

*This is an approximation and would not hold for very large angles. It is, however, good for any situation likely to be encountered in designing highway noise barriers. See pp. 30-34 of "Noise Barrier Screen Measurements, Single Barriers," APL-UW 7509 (Research Report No. 24.1, Washington State Department of Highways), dated June 30, 1975.

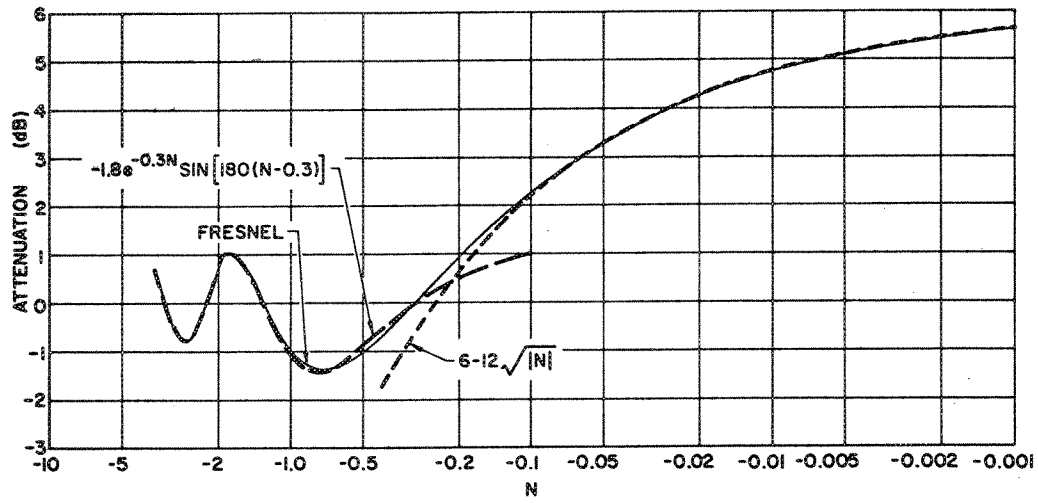

Figure B-1. Approximate formula plots for the case where the wall does not block the line of sight.

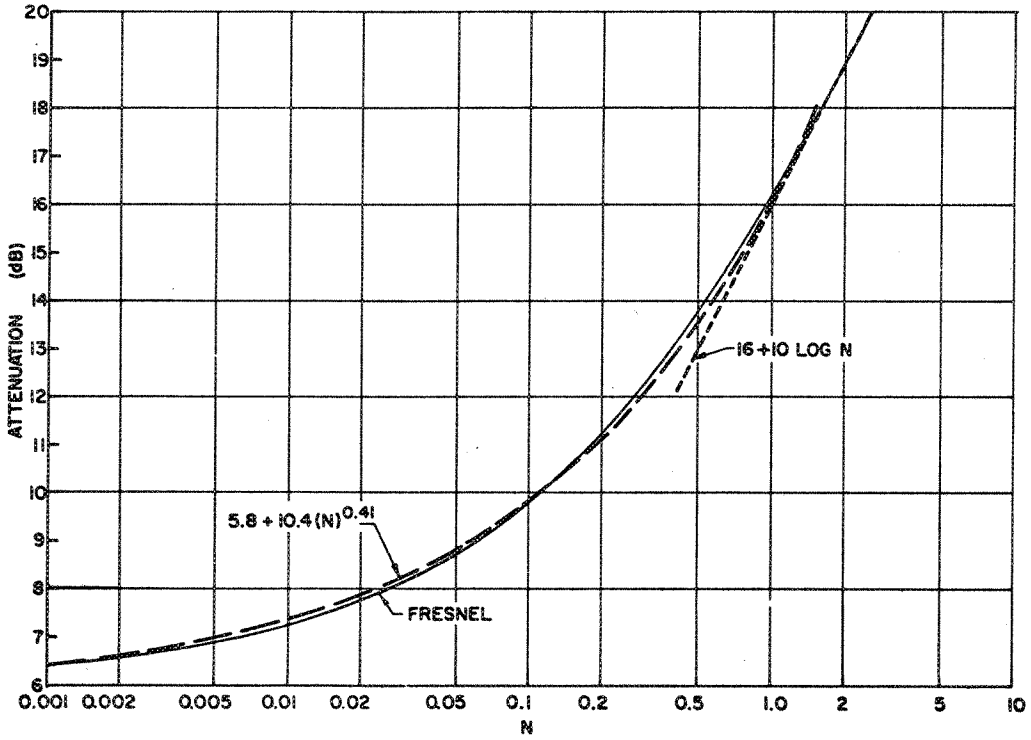

Figure B-2. Approximate formula plots for the case where the wall blocks the line of sight.

Table B-I. Fresnel diffraction.

R	V	dB	N	R	V	dB	N
0.707	0	-6.0	0	0.815	-0.14	- 4.79	-0.01
0.782	-0.1	-5.15	-0.005	0.782	-0.10	- 5.15	-0.005
0.863	-0.2	-4.29	-0.02	0.75	-0.06	- 5.51	-0.0018
0.955	-0.3	-3.41	-0.045	0.736	-0.04	- 5.67	-0.0008
1.045	-0.4	-2.63	-0.08	0.707	0	- 6.0	0
1.14	-0.5	-1.87	-0.125	0.68	+0.04	- 6.36	+0.0008
1.24	-0.6	-1.14	-0.18	0.666	+0.06	- 6.54	+0.0018
1.34	-0.7	-0.47	-0.245	0.64	+0.10	- 6.89	+0.005
1.41	-0.77	0	-0.296	0.614	+0.14	- 7.25	+0.01
1.433	-0.8	+0.11	-0.32	0.58	+0.2	- 7.74	+0.02
1.52	-0.9	+0.63	-0.405	0.526	+0.3	- 8.59	+0.045
1.588	-1.0	+1.01	-0.50	0.478	+0.4	- 9.42	+0.08
1.635	-1.1	+1.26	-0.605	0.436	+0.5	-10.22	+0.125
1.665	-1.2	+1.42(P)	-0.72	0.40	+0.6	-10.97	+0.18
1.645	-1.3	+1.31	-0.845	0.366	+0.7	-11.74	+0.245
1.60	-1.4	+1.07	-0.98	0.336	+0.8	-12.48	+0.32
1.525	-1.5	+0.66	-1.125	0.308	+0.9	-13.24	+0.405
1.430	-1.6	+0.10	-1.28	0.285	+1.0	-13.91	+0.50
1.41	-1.62	0	-1.312	0.265	+1.1	-14.55	+0.605
1.335	-1.7	-0.50	-1.445	0.248	+1.2	-15.12	+0.72
1.265	-1.8	-0.97	-1.62	0.230	+1.3	-15.78	+0.845
1.250	-1.88	-1.07(B)	-1.767	0.218	+1.4	-16.24	+0.98
1.30	-2.0	-0.73	-2.0	0.206	+1.5	-16.73	+1.125
1.41	-2.12	0	-2.247	0.193	+1.6	-17.30	+1.28
1.485	-2.2	+0.42	-2.42	0.183	+1.7	-17.76	+1.445
1.55	-2.33	+0.80(P)	-2.714	0.175	+1.8	-18.15	+1.62
1.54	-2.4	+0.74	-2.88	0.168	+1.9	-18.50	+1.805
1.475	-2.5	+0.37	-3.125	0.158	+2.0	-19.04	+2.0
1.41	-2.56	0	-3.277	For N above 2, use dB = -(16 + 10 log N).			
1.30	-2.7	-0.73	-3.645				

Above line of sight

Below line of sight

(d) For negative values of N greater than -0.22, use

$$-1.8\ e^{-0.3N} \sin\left[180(N-0.3)\right]\ (\text{dB})\ .$$

The sine function is used as though the contents of the brackets were in degrees.

Figures B-1 and B-2 are plots of the Fresnel curve and the curves derived from the preceding equations for positive and negative values, respectively. Note that the results deviate less than 0.2 dB from the Fresnel diffraction curve; in most regions the fit is much closer. The largest deviation occurs at N = -0.22 where, for a very small region, the equations give values that are lower by about 0.4 dB.

APPENDIX C

MEASUREMENT PROCEDURE

When a series of measurements was to be performed, the oscilloscope and other electronics were warmed up well before hand to ensure they had stabilized. The acoustic pulse was then turned on and the oscilloscope adjusted to monitor the microphone from the time the pulse left the source until well after the main pulse had passed. The gain was set very high to examine the trace before the arrival of the first tone burst to ensure that traces of reverberation from previous pulses were not still occurring, and the repetition rate was adjusted accordingly. The gain was then reduced and reverberation subsequent to the main pulse was examined to see if it seemed reasonable in light of the geometries involved. The pulse width was checked both with the wall down and with the wall up to assure that the pulse was as long as possible but was still completely terminated before the arrival of any reverberation from the floor, ceiling, etc.

The sweep on the oscilloscope was switched to X5 magnification and a region in the center of the tone burst where it had leveled off in a "steady state" was centered on the screen. The particular positive-going cycle of the pulse chosen for the actual measurement was then carefully identified by counting the cycles from both ends of the tone burst. The base line of the waveform was then suppressed well below the bottom of the oscilloscope screen and the gain of the oscilloscope was turned up so the tone burst tops were displayed on the scope. This allowed small changes in the amplitude of the waveform to be detected. With the walls removed, the precision decade attenuator was then set and the oscilloscope adjusted so that the peak of the chosen cycle was exactly on one of the horizontal graticule lines of the oscilloscope screen--usually the next to the top line. The walls were then erected and the setting on the decade potentiometer increased (less attenuation) until the selected part of the waveform was again on the reference graticule of the oscilloscope. The difference in the two readings on the precision decade potentiometer was then used to compute the attenuation caused by the presence of the wall. The equation used was $20 \log (A1/A2)$.

As can be seen, we did not depend on the oscilloscope as a calibrated reading instrument; this function was transferred to the highly accurate precision potentiometer. The oscilloscope did not even have to be linear; it did, however, have to remain stable for the period between the two measurements. Our oscilloscope easily met this requirement. When reading the waveform after the walls had been erected, we had to be careful to pick the same part of the tone pulse used for the first measurement, since the pulse was delayed slightly because of the walls. We do not believe we introduced any error in the data from this particular source.

The base line on the oscilloscope was usually sufficiently suppressed and the gain sufficiently high that a 1-dB change (the system was actually linear, not in decibels) in the amplitude of the waveform corresponded to 1 or 2 cm on the face of the oscilloscope. At this resolution, the signal varied slightly from pulse to pulse in a somewhat random manner, with small changes in amplitude occurring over a period of perhaps 1 second and longer-term changes with periods of 5-10 seconds. We verified that these were acoustic (not electronic) phenomena by placing the microphone close to the source while it was transmitting at a fairly high level, in which case the received waveform is quite steady. If the drift had been in the electronics, or transducers, it should have appeared in this experiment as well as in the actual measurements. The base line of the waveform was also checked by displaying it on the oscilloscope screen during conditions when the peaks of the waveform were observed to vary considerably. The base line was relatively steady, indicating that components of the received tone burst amplitude were being modulated rather than an additional signal being applied. The amount of this variability depended on the specific measurement conditions. This variability meant that some operator judgement was required when "nulling" the oscilloscope for an attenuation measurement.

The method used to establish the setting on the precision decade potentiometer was essentially that of "eye averaging." The operator would make a tentative setting and observe the waveform for 20 or 30 seconds to see if the setting was a reasonable value; if not, he would move the potentiometer to a new setting and repeat the observation. This process was continued until the signal appeared to spend as much time above the reference gradicule as it did below it. It would certainly be possible to refine this procedure with more extensive processing; however, the scope of the program was too small to include such refinement at the time.

APPENDIX D

EXPERIMENTAL PARAMETERS

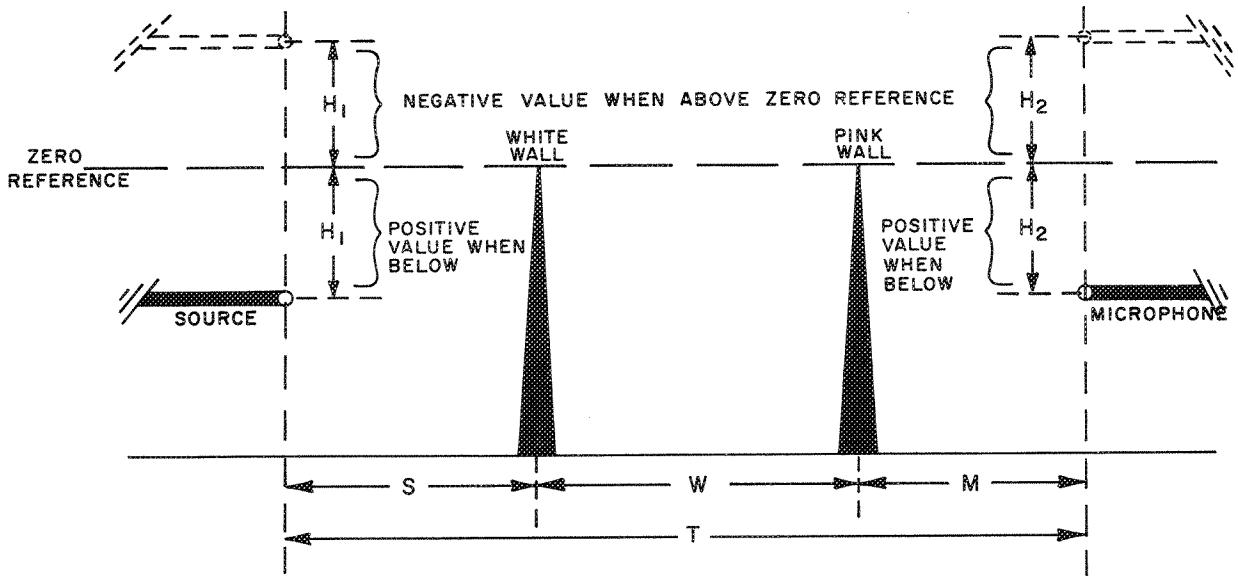

ALL DISTANCES MEASURED IN CENTIMETERS

SERIES EXP. G1
S = 100.0 T = 324.5
W = 78.5 W/T = 0.242
M = 146.0

SERIES EXP. G2
S = 192.0 T = 769.8
W = 186.3 W/T = 0.242
M = 391.5

SERIES EXP. G4
S = 192.0 T = 769.8
W = 28.4 W/T = 0.0369
M = 549.4

SERIES EXP. G5
S = 431.5 T = 769.8
W = 28.4 W/T = 0.0369
M = 309.9

SERIES EXP. G7A
S = 102.7 T = 805.5
W = 28.4 W/T = 0.0353
M = 674.4

SERIES EXP. G8
S = 102.7 T = 428.2
W = 214.5 W/T = 0.501
M = 111.0

SERIES EXP. G9
S = 20.3 T = 257.4
W = 214.1 W/T = 0.832
M = 23.0

SERIES EXP. G9A
S = 35.8 T = 272.9
W = 214.1 W/T = 0.785
M = 23.0

SERIES EXP. G10
S = 191.5 T = 702.9
W = 17.4 W/T = 0.0248
M = 494.0

SERIES EXP. G11
S = 182.5 T = 691.8
W = 71.2 W/T = 0.103
M = 438.1

SERIES EXP. G12
S = 54.6 T = 296.8
W = 193.5 W/T = 0.652
M = 48.7

SERIES EXP. G13
S = 196.5 T = 702.9
W = 7.8 W/T = 0.0111
M = 498.6